

1 **Differential response of macrophages and neutrophils to**
2 **trypanosome infections in zebrafish: occurrence of foamy**
3 **macrophages**

4
5
6
7
8
9

Sem H. Jacobs^{1,2}, Éva Dóró^{1,*}, Ffion R. Hammond^{1,#}, Mai E. Nguyen- Chi³, Georges Lutfalla³, Geert F. Wiegertjes^{1,4}, Maria Forlenza^{1,\$}

10 ¹ Cell Biology and Immunology Group, Department of Animal Sciences, Wageningen University &
11 Research, Wageningen, The Netherlands

12 ² Experimental Zoology Group, Department of Animal Sciences, Wageningen University & Research,
13 Wageningen, The Netherlands

14 ³ DIMNP, CNRS, University of Montpellier, Montpellier, France

15 ⁴ Aquaculture and Fisheries Group, Department of Animal Sciences, Wageningen University &
16 Research, Wageningen, The Netherlands

17
18
19
20

21 * current address: Institute of Physiology, Faculty of Medicine, University of Pécs, Pécs, Hungary

22 # current address: Department of Infection, Immunity & Cardiovascular Disease, University of
23 Sheffield, Sheffield, United Kingdom

24
25

\$: correspondence should be addressed to: maria.forlenza@wur.nl

26 **Abstract**

27

28 A tightly regulated innate immune response to trypanosome infections is critical to strike
29 a balance between parasite control and inflammation-associated pathology. In the present
30 study, we make use of the recently established *Trypanosoma carassii* infection model in
31 larval zebrafish to study the early response of macrophages and neutrophils to
32 trypanosome infections *in vivo*. We consistently identified high- and low-infected
33 individuals and were able to simultaneously characterize their differential innate response.
34 Not only did macrophage and neutrophil number and distribution differ between the two
35 groups, but also macrophage morphology and activation state. Exclusive to high-infected
36 zebrafish, was the appearance of macrophages rich in lipid droplets, confirmed to be foamy
37 macrophages and characterized by a strong pro-inflammatory profile. Altogether, we
38 provide an *in vivo* characterization of the differential response of macrophage and
39 neutrophil to trypanosome infection and identify foamy macrophages as potentially
40 associated with an exacerbated immune response and susceptibility to the infection. To
41 our knowledge this is the first report of the occurrence of foamy macrophages during an
42 extracellular trypanosome infection.

43 **Introduction**

44

45 Trypanosomes of the *Trypanosoma* genus are protozoan haemoflagellates that can infect
46 animals from all vertebrate classes, including warm-blooded mammals and birds as well
47 as cold-blooded amphibians, reptiles and fish. This genus contains human and animal
48 pathogens, including the intracellular *Trypanosoma cruzi* (causing Human American
49 Trypanosomiasis or Chagas' disease), the extracellular *T. brucei rhodesiense* and *T. brucei*
50 *gambiense* (causing Human African Trypanosomiasis or Sleeping Sickness) and *T.*
51 *congolense*, *T. vivax* and *T. b. brucei* (causing Animal African Trypanosomiasis or Nagana)
52 (Radwanska et al., 2018; Simpson et al., 2006). Among these, salivarian trypanosomes
53 such as *T. brucei* ssp. live extracellularly in the bloodstream or tissue fluids of their host.
54 For example, *T. vivax* can multiply rapidly and is evenly distributed throughout the
55 cardiovascular system, *T. congolense* tends to aggregate in small blood vessels, whereas
56 *T. brucei* especially can extravasate and multiply in interstitial tissues (reviewed by Magez
57 and Caljon, 2011). Pathologically, anaemia appears to be a factor common to infections
58 with most if not all trypanosomes although with different underlying causative
59 mechanisms. These include, among others, erythrophagocytosis by macrophages (Cnops
60 et al., 2015; Guegan et al., 2013), hemodilution (Naessens, 2006), erythrolysis through
61 intermembrane transfer of variant surface glycoprotein (VSG) from trypanosomes to
62 erythrocytes (Rifkin and Landsberger, 1990), oxidative stress from free radicals (Mishra et
63 al., 2017) and mechanical damage through direct interaction of trypanosomes with
64 erythrocytes surface (Boada-Sucre et al., 2016).

65 Immunologically, infections with trypanosomes are often associated with dysfunction and
66 pathology related to exacerbated innate and adaptive immune responses (reviewed by
67 Radwanska et al., 2018; Stijlemans et al., 2016). Initially it was believed that antibody-
68 dependent complement-mediated lysis was the major protective mechanism involved in
69 early parasite control (Krettli et al., 1979; Musoke and Barbet, 1977). However, later
70 studies revealed that at low antibody levels, trypanosomes can efficiently remove surface-
71 bound antibodies through an endocytosis-mediated mechanisms (Engstler et al., 2007),
72 and that complement C5-deficient mice are able to control the first-peak parasitaemia
73 similarly to wild type mice (La Greca et al., 2014). Instead, innate immune mediators such
74 as IFN γ , TNF α and nitric oxide (NO) were shown to be indispensable for the control of first-
75 peak parasitaemia, through direct and indirect mechanisms (reviewed by Radwanska et
76 al., 2018). In the early phase of infection, the timely induction of IFN γ by NK, NKT and
77 CD8 $^{+}$ cells (Cnops et al., 2015) followed by the production of TNF α and NO by IFN γ -primed
78 macrophages (Baral et al., 2007; Iraqi et al., 2001; Lopez et al., 2008; Rudolf Lucas et al.,
79 1994; Magez et al., 1993, 2007, 2006, 2001, 1999; O'Gorman et al., 2006; Sternberg and
80 Mabbott, 1996; Wu et al., 2017) leads to effective control of first-peak parasitaemia.

Macrophages and neutrophils response to trypanosome infections in zebrafish

81 Glycosyl-inositol-phosphate soluble variant surface glycoproteins (GPI-VSG) released from
82 the surface of trypanosomes were found to be the major inducers of TNF α in macrophages,
83 and that such response could be primed by IFN γ (Coller et al., 2003; Magez et al., 2002).
84 When macrophages would encounter GPI-VSG prior to IFN γ exposure however, their TNF α
85 and NO response would dramatically be reduced (Coller et al., 2003) which, depending on
86 the timing, could either lead to macrophage unresponsiveness or prevent exacerbated
87 inflammatory responses during the first-peak of parasite clearance. Altogether, these data
88 made clear that an early innate immune response is crucial to control the acute phase of
89 trypanosome infection, but that its tight regulation is critical to ensure parasite control as
90 opposed to pathology.

91 All the findings above took advantage of the availability of several mice models for
92 trypanosome infection using trypanosusceptible or trypanotolerant as well as mutant
93 'knock-out' mice strains. Although mice cannot be considered natural hosts of
94 trypanosomes and do not always recapitulate all features of natural infections, the
95 availability of such models allowed to gain insights into the general biology of
96 trypanosomes, their interaction with and evasion of the host immune system, as well as
97 into various aspects related to vaccine failure, antigenic variation, and (uncontrolled)
98 inflammation (Magez and Caljon, 2011). The use of knock-out strains for example, shed
99 specific light on the role of various cytokines, particularly TNF α , IFN γ and IL-10, in the
100 control of parasitaemia and in the induction of pathological conditions during infection
101 (reviewed in Magez and Caljon, 2011). It would be ideal to be able to follow, *in vivo*, the
102 early host responses to the infection and visualise the trypanosome response to the host's
103 attack. However, due to the lack of transparency of most mammalian hosts, this has not
104 yet been feasible.

105 We recently reported the establishment of an experimental trypanosome infection of
106 zebrafish (*Danio rerio*) with the fish-specific trypanosome *Trypanosoma carassii* (Dóro et
107 al., 2019). In the latter study, by combining *T. carassii* infection of transparent zebrafish
108 with high-resolution high-speed microscopy, we were able to describe in detail the
109 swimming behaviour of trypanosomes *in vivo*, in the natural environment of blood and
110 tissues of a live vertebrate host. This led to the discovery of novel attachment mechanisms
111 as well as trypanosome swimming behaviours that otherwise would not have been
112 observed *in vitro* (Dóro et al., 2019). Previous studies in common carp (*Cyprinus carpio*),
113 goldfish (*Carrassius aurata*) and more recently zebrafish, demonstrated that infections with
114 *T. carassii* present many of the pathological features observed during human or animal
115 trypanosomiasis, including a pro-inflammatory response during first-peak parasitaemia
116 (Kovacevic et al., 2015; Oladiran et al., 2011; Oladiran and Belosevic, 2009) polyclonal B
117 and T cell activation (Joerink et al., 2007, 2004; Lischke et al., 2000; Ribeiro et al., 2010;
118 Woo and Ardelli, 2014) and anaemia (Dóro et al., 2019; Islam and Woo, 1991; McAllister

Macrophages and neutrophils response to trypanosome infections in zebrafish

119 et al., 2019). These shared features among human and animal (including fish)
120 trypanosomiases suggest a commonality in (innate) immune responses to trypanosomes
121 across different vertebrates.

122 Zebrafish are fresh water cyprinid fish closely related to many of the natural hosts of *T.*
123 *carassii* (Kent et al., 1993; Simpson et al., 2006) and are a powerful model species owing
124 to, among others, their genetic tractability, large number of transgenic lines marking
125 several immune cell types, knock-out mutant lines and most importantly, the transparency
126 of developing embryos allowing high-resolution *in vivo* visualisation of cell behaviour
127 (Benard et al., 2015; Bertrand et al., 2010; Ellett et al., 2011; Langenau et al., 2004;
128 Lawson and Weinstein, 2002; Page et al., 2013; Petrie-Hanson et al., 2009; Renshaw et
129 al., 2006; White et al., 2008). During the first 2-3 weeks of development, zebrafish are
130 devoid of mature T and B lymphocytes and thus offer a window of opportunity to study
131 innate immune responses (Torraca et al., 2014; Torraca and Mostowy, 2018), especially
132 those driven by neutrophils and macrophages. The response of macrophages and
133 neutrophilic granulocytes towards several viral, fungal and bacterial pathogens has been
134 studied in detail using zebrafish (Cronan and Tobin, 2014; García-Valtanen et al., 2017;
135 Nguyen-Chi et al., 2014a; Palha et al., 2013; Ramakrishnan, 2013; Renshaw and Trede,
136 2012; Rosowski et al., 2018; Torraca and Mostowy, 2018) but never before in the context
137 of trypanosome infections.

138 Taking advantage of the recently established zebrafish-*T. carassii* infection model and of
139 the availability of zebrafish transgenic lines marking macrophages and neutrophils as well
140 as *il1b*- and *tnfa*-expressing cells, in the current study, we describe the early events of the
141 innate immune response of zebrafish to *T. carassii* infections. Based on a novel clinical
142 scoring system relying, amongst other criteria, on *in vivo* real-time monitoring of
143 parasitaemia, we could consistently segregate larvae in high- and low-infected individuals
144 without having to sacrifice the larvae. Between these individuals we always observed a
145 marked differential response between macrophages and neutrophils, especially with
146 respect to their proliferative capacity and redistribution in tissues or major blood vessels
147 during infection. Significant differences were observed in the inflammatory response of
148 macrophages in high- and low-infected individuals and in their susceptibility to the
149 infection. In low-infected individuals, despite an early increase in macrophage number, a
150 mild inflammatory response strongly associated with control of parasitaemia and survival
151 to the infection was observed. Conversely, exclusively in high-infected individuals, we
152 describe the occurrence of large, granular macrophages, reminiscent of foamy
153 macrophages (Vallochi et al., 2018), characterized by a strong inflammatory profile and
154 association to susceptibility to the infection. This is the first report of the occurrence of
155 foamy macrophages during an extracellular trypanosome infection.

156 **Materials and methods**

157

158 **Zebrafish lines and maintenance**

159 Zebrafish were kept and handled according to the Zebrafish Book (zfin.org) and local
160 animal welfare regulations of The Netherlands. Zebrafish embryo and larvae were raised
161 in egg water (0.6 g/L sea salt, Sera Marin, Heinsberg, Germany) at 27°C with a 12:12
162 light-dark cycle. From 5 days post fertilisation (dpf) until 14 dpf larvae were fed
163 Tetrahymena once a day. From 10 dpf larvae were also daily fed dry food ZM-100 (ZM
164 systems, UK). The following zebrafish lines used in this study: transgenic *Tg(mpx:GFP)¹¹⁴*
165 (Renshaw et al., 2006), *Tg(kdrl:hras-mCherry)^{s896}* referred as *Tg(kdrl:caax-mCherry)* (Chi
166 et al., 2008), *Tg(fli1:eGFP)^{v1}* (Lawson and Weinstein, 2002), *Tg(mpeg1:eGFP)^{g122}* (Ellett et
167 al., 2011), *Tg(mpeg1.4:mCherry-F)^{ump2Tg}*, *Tg(il1b:eGFP-F)^{ump3Tg}*, (Nguyen-Chi et al.,
168 2014b), *Tg(tnfa:eGFP-F)^{ump5Tg}* (Nguyen-Chi et al., 2015) or crosses thereof. The latter
169 three transgenic zebrafish lines express a farnesylated (membrane-bound) mCherry
170 (mCherry-F) or eGFP (eGFP-F) under the control of the *mpeg1*, *il1b* or *tnfa* promoter,
171 respectively.

172 **Trypanosoma carassii culture and infection of zebrafish larvae**

173 *Trypanosoma carassii* (strain TsCc-NEM) was cloned and characterized previously (Overath
174 et al., 1998) and maintained in our laboratory by syringe passage through common carp
175 (*Cyprinus carpio*) as described previously (Dóro et al., 2019). Blood was drawn from
176 infected carp and kept at 4°C overnight in siliconized tubes. Trypanosomes enriched at the
177 interface between the red blood cells and plasma were collected and centrifuged at 800 xg
178 for 8 min at room temperature. Trypanosomes were resuspended at a density of 5 x 10⁵-
179 1 x 10⁶ ml and cultured in 75 or 165 cm² flasks at 27°C without CO₂ in complete medium
180 as described previously (Dóro et al., 2019). *T. carassii* were kept at a density below 5 x
181 10⁶/ml, and sub-cultured 1-3 times a week. In this way *T. carassii* could be kept in culture
182 without losing infectivity for up to 2 months. The majority of carp white blood cells present
183 in the enriched trypanosome fraction immediately after isolation, died within the first 3-5
184 days of culture and any remaining blood cell was removed prior to *T. carassii* injection into
185 zebrafish. To this end, cells were centrifuged at 800 xg for 5 min in a 50 ml Falcon tube
186 and the tube was subsequently tilted in a 20° angle in relation to the table surface,
187 facilitating the separation of the motile trypanosomes along the conical part of the tube
188 from the static pellet of white blood cells at the bottom of the tube.
189 For zebrafish infection, trypanosomes were cultured for 1 week and no longer than 3
190 weeks. Infection of zebrafish larvae was performed as described previously (Dóro et al.,
191 2019). Briefly, prior to injection, 5 days post fertilization (dpf) zebrafish larvae were
192 anaesthetized with 0.017% Ethyl 3-aminobenzoate methanesulfonate (MS-222, Tricaine,

Macrophages and neutrophils response to trypanosome infections in zebrafish

193 Sigma-Aldrich) in egg water. *T. carassii* were resuspended in 2% polyvinylpyrrolidone
194 (PVP, Sigma-Aldrich) and injected (n=200) intravenously in the Duct of Cuvier.

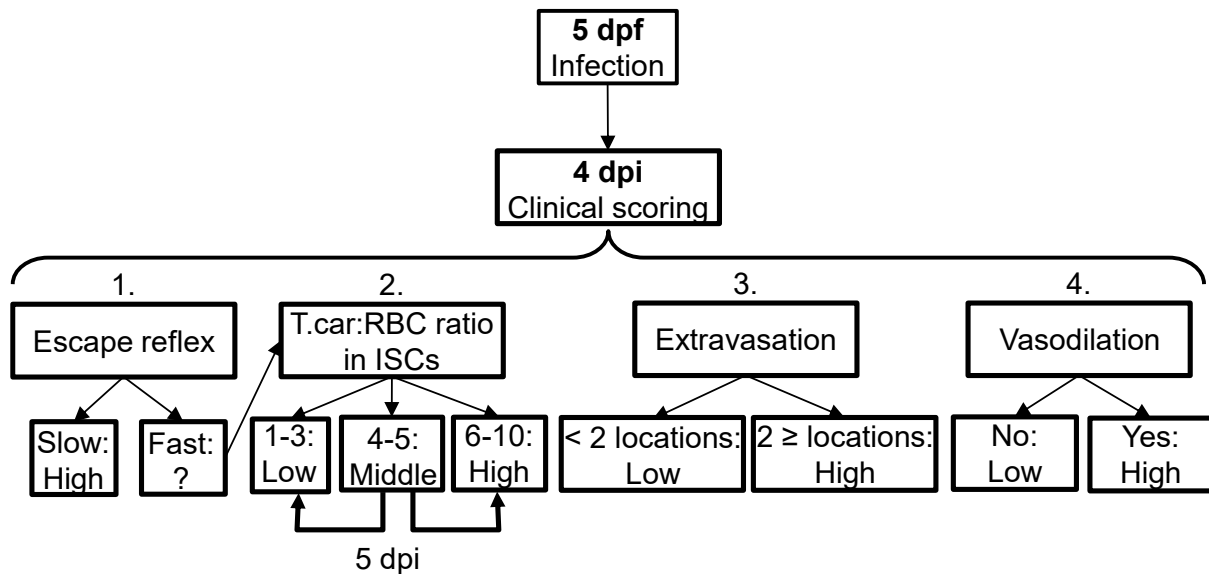
195

196 **Clinical scoring system of the severity of infection**

197 Careful monitoring of the swimming behaviour of zebrafish larvae after infection (5 dpf
198 onwards) as well as *in vivo* observation of parasitaemia development in transparent larvae,
199 led to the observation that from 4 days post infection (dpi) onwards larvae could generally
200 be segregated into high- and low-infected individuals. To objectively assign zebrafish to
201 either one of these two groups, we developed a clinical scoring system (**Fig 1**). The first
202 criterion looked at the escape reflex upon contact with a pipette and was sufficient to
203 identify high-infected individuals as those not reacting to the pipet (slow swimmers). To
204 categorize the remaining individuals, an infection score based on counting parasite: blood
205 cell ratios in 100 events passing through the intersegmental capillary (ISC) above the
206 cloaca was developed. The infection scores on a scale from 1 to 10 were assigned as
207 follows: 1=no parasites observed, 2=1-10% parasite, 3=11-20% parasite, 4=21-30%
208 parasite, 5=31-40% parasite, 6=41-55% parasite, 7=56-70% parasite, 8=71-85%
209 parasite, 9=86-99%, 10=no blood cells observed. Larvae with infection scores between 1-
210 3 were categorized as low-infected while scores between 6-10 were categorized as high
211 infected. Larvae with scores 4-5 were reassessed 1 day later, at 5 dpi, and then categorised
212 as high- or low-infected. Next to that, the swimming behaviour of larvae was observed and
213 compared to the control group. Heartbeat of the larvae was monitored and noted if it was
214 slower than the control. The diameter of the cardinal caudal vein in the trunk area after
215 the cloaca region was measured in ImageJ 1.49o to quantify the degree of vasodilation.
216 Eventual blockage of tail tip vessel-loop was also noted. Extravasation and the location of
217 extravasated parasites (e.g. fins, muscle, intraperitoneal cavity, and interstitial space lining
218 the blood vessels) was recorded.

219

Macrophages and neutrophils response to trypanosome infections in zebrafish



220

221 **Fig 1. Schematic overview of the clinical scoring system used to determine individual**
222 **infection levels of *T. carassii*-infected zebrafish larvae.**

223 Zebrafish larvae infected with *T. carassii* can be analysed at 4 dpi; based on up to 4 different
224 parameters including 1) visual monitoring of larval behaviour, 2) parasite numbers, 3) location
225 or 4) vasodilation, larvae could be segregated into high- and low-infected individuals. See
226 details in the text in the corresponding Materials & Methods section.

227

228 **Real-time quantitative PCR**

229 Zebrafish were sacrificed by an overdose of MS-222 anaesthetic (50 mg/L). At each time
230 point 3-6 zebrafish larvae were sacrificed and pooled. Pools were transferred to RNA later
231 (Ambion), kept at 4°C overnight and then transferred to -20°C for further storage. Total
232 RNA isolation was performed with the Qiagen RNeasy Micro Kit (QIAGEN, Venlo, The
233 Netherlands) according to manufacturer's protocol. Next, 250-500 ng total RNA was used
234 as template for cDNA synthesis using SuperScript III Reverse Transcriptase and random
235 hexamers (Invitrogen, Carlsbad, CA, USA), following the manufacturer's instructions with
236 an additional DNase step using DNase I Amplification Grade (Invitrogen, Carlsbad, CA,
237 USA). cDNA was then diluted 25 times to serve as template for real-time quantitative PCR
238 (RT-qPCR) using Rotor-Gene 6000 (Corbett Research, QIAGEN), as previously described
239 (Forlenza et al., 2012). Primers for *ef1a*: FW-CTGGAGGCCAGCTCAAACAT, RV-
240 TCAAGAAGAGTAGTAGTACCG (ZDB-GENE-990415-52); *T. car. hsp70*: FW-
241 CAGCCGGTGGAGCGCGT, RV-AGTTCCTTGCCGCGGAAGA (FJ970030.1, GeneBank) were
242 obtained from Eurogentec (Liège, Belgium). Gene expression was normalized to the
243 expression of *elongation factor-1 alpha (ef1a)* housekeeping gene and expressed relative
244 to the PVP control at the same time point or to 0 days post injection (dpi) time point.

245

246 **In vivo imaging and videography of zebrafish**

247 Prior to imaging, zebrafish larvae were anaesthetised with 0.017% MS-222 (Sigma-
248 Aldrich). For total fluorescence acquisition, double transgenic *Tg(mpeg1.4:mCherry-
249 F;mpx:GFP)* were positioned on preheated flat agar plates (1% agar in egg water with

Macrophages and neutrophils response to trypanosome infections in zebrafish

250 0.017% MS-222) and imaged with Fluorescence Stereo Microscope (Leica M205 FA). The
251 image acquisition settings were as following: Zoom: 2.0 - 2.2, Gain: 1, Exposure time
252 (ms): 70 (BF)/700 (GFP)/1500 (mCherry), Intensity: 60 (BF)/700 (GFP)/700 (mCherry),
253 Contrast: 255/255 (BF)/ 70/255 (GFP)/ 15/255 (mCherry).

254 Alternatively, anaesthetised larvae were embedded in UltraPure LMP Agarose (Invitrogen)
255 and positioned on the coverglass of a 35 mm petri dish, (14 mm microwell, coverglass No.
256 0 (0.085-0.13mm), MatTek corporation) prior to imaging. A Roper Spinning Disk Confocal
257 (Yokogawa) on Nikon Ti Eclipse microscope with 13x13 Photometrics Evolve camera (512
258 x 512 Pixels 16 x 16 micron) equipped with a 40x (1.30 NA, 0.24 mm WD) OI objective,
259 was used with the following settings: GFP excitation: 491nm, emission: 496-560nm,
260 digitizer: 200 MHz (12-bit); 561 BP excitation: 561nm; emission: 570-620nm, digitizer:
261 200 MHz (12-bit); BF: digitizer: 200 MHz (12-bit). Z-stacks of 1 or 0.5 μ m. An Andor-
262 Revolution Spinning Disk Confocal (Yokogawa) on a Nikon Ti Eclipse microscope with Andor
263 iXon888 camera (1024 x 1024 Pixels 13 x 13 micron) equipped with 40x (0.75 NA, 0.66
264 mm WD) objective, 40x (1.15 NA, 0.61-0.59 mm WD) WI objective, 20x (0.75 NA, 1.0
265 mm WD) objective and 10x (0.50 NA, 16 mm WD) objective was used with the following
266 settings: Dual pass 523/561: GFP excitation: 488nm, emission: 510-540nm, EM gain: 20-
267 300ms, digitizer: 10 MHz (14-bit); RFP excitation: 561nm; emission: 589-628nm, EM gain:
268 20-300ms, digitizer: 10 MHz (14-bit); BF DIC EM gain: 20-300ms, digitizer: 10 MHz (14-
269 bit). Z-stacks of 1 μ m. Images were analysed with ImageJ-Fijii (version 1.52p).

270 High-speed videography of *T. carassii* swimming behaviour *in vivo* was performed as
271 described previously (Dóro et al., 2019). Briefly, the high-speed camera was mounted on
272 a DMi8 inverted digital microscope (Leica Microsystems), controlled by Leica LASX software
273 (version 3.4.2.) and equipped with 40x (NA 0.6) and 20x (NA 0.4) long distance objectives
274 (Leica Microsystems). For high-speed light microscopy a (8 bits) EoSens MC1362
275 (Mikrotron GmbH, resolution 1280 x 1024 pixels), with Leica HC 1x Microscope C-mount
276 Camera Adapter, was used, controlled by XCAP-Std software (version 3.8, EPIX inc.).
277 Images were acquired at a resolution of 900 x 900 or 640 x 640 pixels. Zebrafish larvae
278 were anaesthetised with 0.017% MS-222 and embedded in UltraPure LMP Agarose
279 (Invitrogen) on a microscope slide (1.4-1.6 mm) with a well depth of 0.5-0.8 mm (Electron
280 Microscopy Sciences). Upon solidification of the agarose, the specimen was covered with
281 3-4 drops of egg water containing 0.017% MS-222, by a 24 x 50 mm coverslip and imaged
282 immediately. For all high-speed videography, image series were acquired at 480-500
283 frames per second (fps) and analysed using a PFV software (version 3.2.8.2) or MiDAS
284 Player v5.0.0.3 (Xcite, USA).

285

286 **Fluorescence quantification**

287 Quantification of total cell fluorescence in zebrafish larvae was performed in ImageJ

Macrophages and neutrophils response to trypanosome infections in zebrafish

288 (version 1.49o) using the free-form selection tool and by accurately selecting the larvae
289 area. Owing to the high auto-fluorescence of the gut or gut content, and large individual
290 variation, the gut area was excluded from the total fluorescence signal. Area integrated
291 intensity and mean grey values of each selected larva were measured by the software. To
292 correct for the background, three consistent black areas were selected in each image.
293 Analysis was performed using the following formula: corrected total cell fluorescence
294 (CTCF) = Integrated density - (Area X Mean background value).

295

296 **EdU proliferation assay and immunohistochemistry**

297 iCLICK™ EdU (5- ethynyl-2'- deoxyuridine, component A) from ANDY FLUOR 555 Imaging
298 Kit (ABP Biosciences) at a stock concentration of 10 mM, was diluted in PVP to 1.13 mM.
299 Infected *Tg(mpeg1:eGFP)* or *Tg(mpx:GFP)* larvae were injected in the heart cavity at 3 dpi
300 (8dpf) with 2 nl of solution, separated in high- and low-infected individuals at 4 dpi and
301 euthanized 6-8 hours later (30-32h after EdU injection) with an overdose of anaesthetic
302 (0.4% MS-222 in egg water). Following fixation in 4% paraformaldehyde (PFA, Thermo
303 Scientific) in PBS, o/n at 4°C, larvae were washed three times in buffer A (0.1% (v/v)
304 tween-20, 0.05% (w/v) azide in PBS), followed by dehydration: 50% MeOH in PBS, 80%
305 MeOH in H₂O and 100% MeOH, for 15 min each, at room temperature (RT), with gentle
306 agitation. To remove background pigmentation, larvae were incubated in bleach solution
307 (5% (v/v) H₂O₂ and 20% (v/v) DMSO in MeOH) for 1h at 4°C, followed by rehydration:
308 100% MeOH, 80% MeOH in H₂O, 50% MeOH in PBS for 15 min each, at room temperature
309 (RT), with gentle agitation. Next, larvae were incubated three times for 5 min each in
310 buffer B (0.2%(v/v) triton-x100, 0.05% azide in PBS) at RT with gentle agitation followed
311 by incubation in EdU iCLICK™ development solution for 30 min at RT in the dark and three
312 rapid washes with buffer B.

313 The described EdU development led to loss of GFP signal in the transgenic zebrafish.
314 Therefore, to retrieve the position of neutrophils or macrophages, wholemount
315 immunohistochemistry was performed. Larvae were blocked in 0.2% triton-x100, 10%
316 DMSO, 6% (v/v) normal goat serum and 0.05% azide in PBS, for 3h, at RT with gentle
317 agitation. Next, the primary antibody Chicken anti-GFP (Aves labs.Inc., 1:500) in Antibody
318 buffer (0.2% tween-20, 0.1% heparin, 10% DMSO, 3% normal goat serum and 0.05%
319 azide in PBS) was added and incubated overnight (o/n) at 37°C. After three rapid and
320 three 5 min washes in buffer C (0.1% tween-20, 0.1% (v/v) heparin in PBS), at RT with
321 gentle agitation, the secondary antibody goat anti-chicken-Alexa 488 (Abcam, 1:500) was
322 added in Antibody buffer and incubated o/n at 37°C. After three rapid and three 5 min
323 washes in buffer C, at RT with gentle agitation, larvae were imaged with Andor Spinning
324 Disk Confocal Microscope.

325

Macrophages and neutrophils response to trypanosome infections in zebrafish

326 **BODIPY injection**

327 BODIPY™ FL pentanoic acid (BODIPY-FL5, Invitrogen) was diluted in DMSO to a 3 mM stock
328 solution. Stock solution was diluted 100x (30 µM) with PVP. Infected larvae 3 dpi (8 dpf)
329 were injected with 1 nl of the solution i.p. (heart cavity) and imaged 18-20 hours later.

330

331 **Statistical analysis**

332 Analysis of gene expression and total fluorescence data were performed in GraphPad
333 PRISM 5. Statistical analysis of gene expression data was performed on Log(2) transformed
334 values followed by One-way ANOVA and Dunnett's multiple comparisons test. Analysis of
335 Corrected Total Cell Fluorescence was performed on Log(10) transformed values followed
336 by Two-way ANOVA and Bonferroni multiple comparisons post-hoc test. Analysis of EdU⁺
337 macrophages was performed on Log(10) transformed values followed by One-way ANOVA
338 and Bonferroni multiple comparisons post-hoc test. In all cases, $p < 0.05$ was considered
339 significant.

Macrophages and neutrophils response to trypanosome infections in zebrafish

340 **Results**

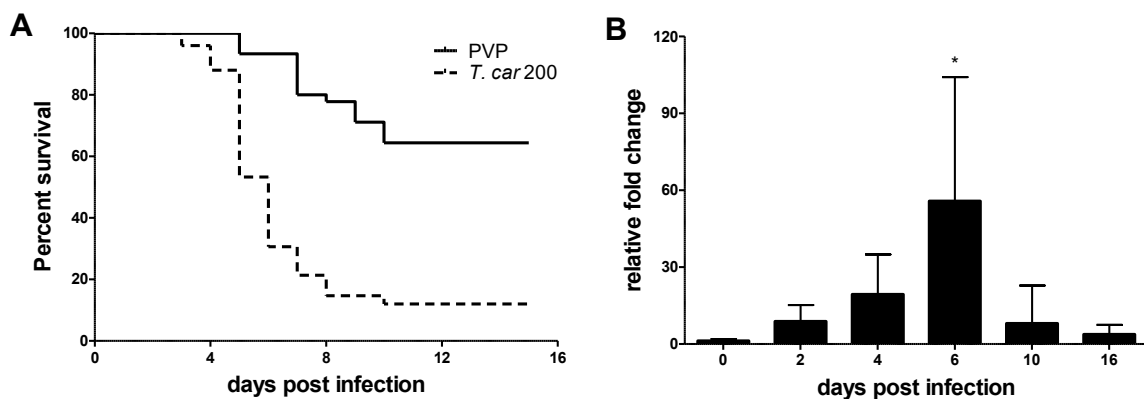
341

342 **Susceptibility of zebrafish larvae to *T. carassii* infection**

343 We recently reported the establishment of a trypanosome infection in zebrafish larvae
344 using a natural fish parasite, *Trypanosoma carassii* (Dóro et al., 2019). To further
345 investigate the immune response to *T. carassii* infection, we first investigated the kinetics
346 of susceptibility of zebrafish larvae as well as the kinetics of expression of various immune-
347 related genes. Similar to the previous report, *T. carassii* infection of 5 dpf zebrafish larvae
348 leads to approximately 10-20% survival by 15 days post infection (dpi) with the highest
349 incidence of mortality between 4 and 7dpi (**Fig 2A**). The onset of mortality coincided with
350 the peak of parasitaemia as assessed by real-time quantitative gene expression analysis
351 of a *T. carassii*-specific gene (**Fig 2B**). Nevertheless, we consistently observed 10-20%
352 survival in the *T. carassii*-infected group, suggesting that zebrafish larvae can control *T.*
353 *carassii* infection. This observation prompted us to investigate the kinetics of parasitaemia
354 and development of (innate) immune responses at the individual level.

355

356



357

358

359 **Fig 2. *T. carassii* infection of larval zebrafish.**

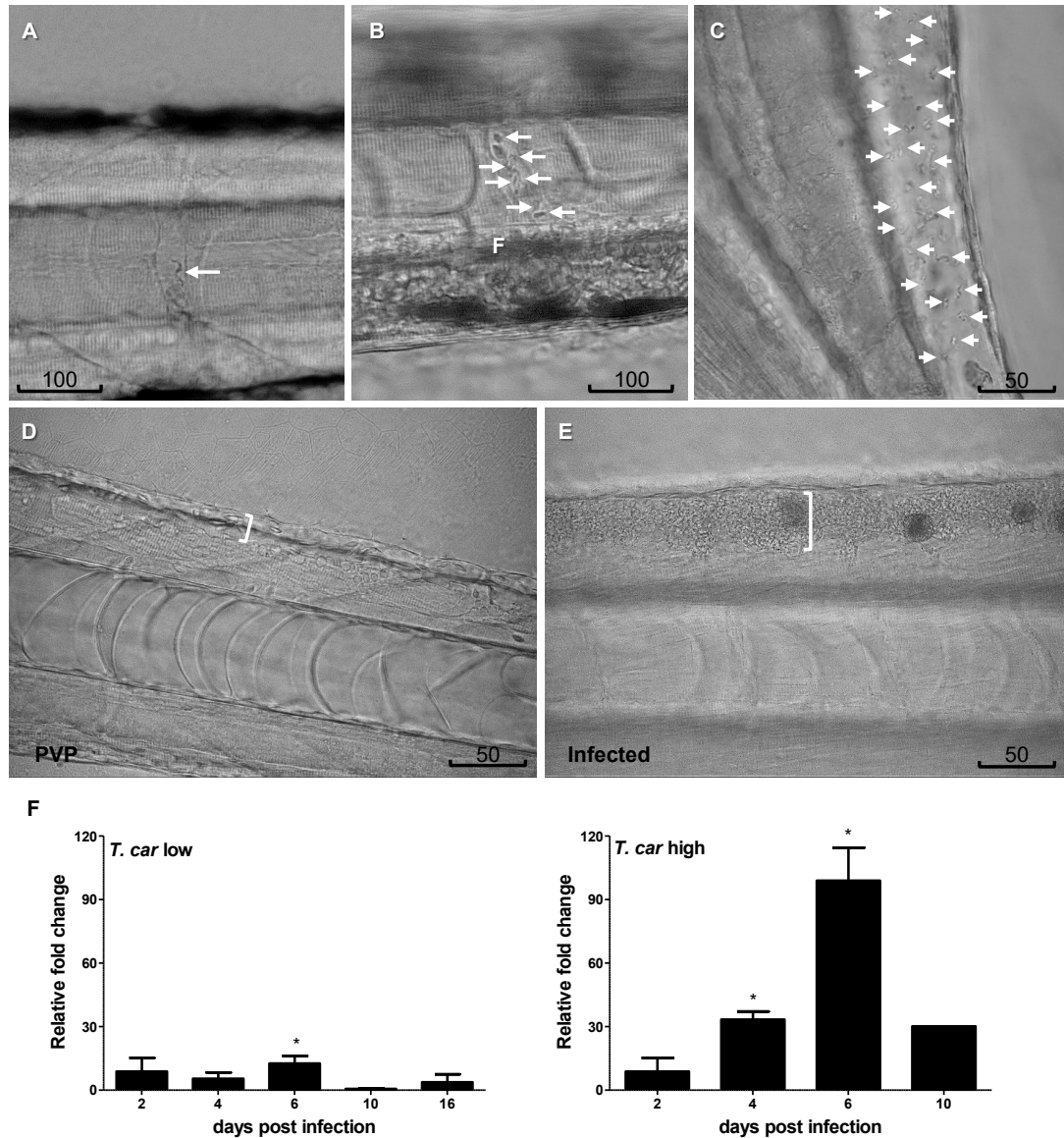
360 **A)** *Tg(mpeg1.4:mCherry-F;mpx:GFP)* larvae (5 dpf) were injected intravenously with $n=200$ *T.*
361 *carassii*/fish or with PVP as control and survival was monitored over a period of 15 days. **B)**
362 *Tg(mpeg1.4:mCherry-F;mpx:GFP)* zebrafish (5 dpf) were treated as in A and sampled at
363 various time points. At each time point, 3-6 pools of 3-5 larvae were sampled for real-time
364 quantitative PCR analysis. Relative fold change of the *T. carassii*-specific *heat-shock protein-70*
365 (*hsp70*) was normalised to the zebrafish-specific *ef1a* and expressed relative to the parasite
366 injected group at time point 0h. Bars indicate average and standard deviation (SD) on $n=3-6$
367 pools per time point.

368 **Clinical signs of *T. carassii* infection and clinical scoring system**

369 To characterize the response to *T. carassii* infection in individual zebrafish larvae, we
370 developed a clinical scoring system to determine individual infection levels, enabling us to
371 group individual larvae based on severity of infection. From 4 dpi onwards, we could
372 consistently sort larvae into groups of high- or low-infected individuals based on *in vivo*
373 observations, without the need to sacrifice animals (**S1 Video**). Infection levels were
374 categorised using four criteria: 1) escape reflex (slow vs fast) upon contact with a pipette
375 tip, 2) infection scores (1-10, see details in Materials and Methods), based on the ratio of
376 blood cells and parasites passing through an intersegmental capillary (ISC) in 100 events
377 (**Fig 3A, 3B**) (**S1 Video**, 00:06-00:39 sec), 3) extravasation, based on the presence of
378 parasites outside of blood vessels (**Fig 3C**) (**S1 Video**, 00:40-1:20 sec) and 4)
379 vasodilation, based on the diameter of the cardinal caudal vein (**Fig 3D, 3E**). The first
380 criterion defined all individuals with a minimal escape reflex (slow swimmers) as high-
381 infected individuals: they were mostly located at the bottom of the tank and showed
382 minimal reaction upon direct contact with a pipette. Larvae with a normal escape reflex
383 (fast swimmers) however, were not exclusively low-infected individuals. Therefore, a
384 second criterion was used based on trypanosome counting in ISC (**S1 Video**, 00:06-00:39
385 sec). Individuals with an infection score between 1-3 were categorized as low-infected and
386 always survived the infection (see Materials and Methods). Individuals with an infection
387 score between 6-10 were categorized as high-infected and generally succumbed to the
388 infection. Individuals with an intermediate score (4-5) could go both ways: they either
389 showed a delayed parasitaemia and later developed high parasitaemia (common) or
390 recovered from the infection (rare). The third criterion clearly identified high-infected
391 individuals as those showing extensive extravasation at two or more of the following
392 locations: peritoneal cavity (**Fig 3C**) (**S1 Video**, 00:40-00:59 sec), interstitial space lining
393 the blood vessels, muscle tissue (**S1 Video**, 01:00-01:07 sec) or fins (**S1 Video**, 01:08-
394 01:20 sec), in particular the anal fin. At these locations, in high-infected individuals,
395 trypanosomes could accumulate in high numbers, filling up all available spaces.
396 Extravasation however could also occur in low-infected individuals, but to a lesser extent.
397 The fourth criterion, vasodilation of the cardinal caudal vein associated with high numbers
398 of trypanosomes in the blood vessels, was a definitive sign of high infection level, and
399 never occurred in low-infected larvae. To validate our scoring system, expression of a *T.*
400 *carassii*-specific gene was analysed in pools of larvae classified as high- or low-infected.
401 As expected, in individuals categorized as high-infected, *T. carassii*-specific gene
402 expression increased more than 60-fold whereas in low-infected individuals the increase
403 was less than 20-fold (**Fig 3F**). Altogether these data show that *T. carassii* infects zebrafish
404 larvae, but that the infection can develop differently among individuals, leading to different
405 outcomes. The clinical scoring system based on numerous criteria is suitable to reliably

Macrophages and neutrophils response to trypanosome infections in zebrafish

406 separate high- and low-infected larvae to further investigate individual immune responses.
407
408
409



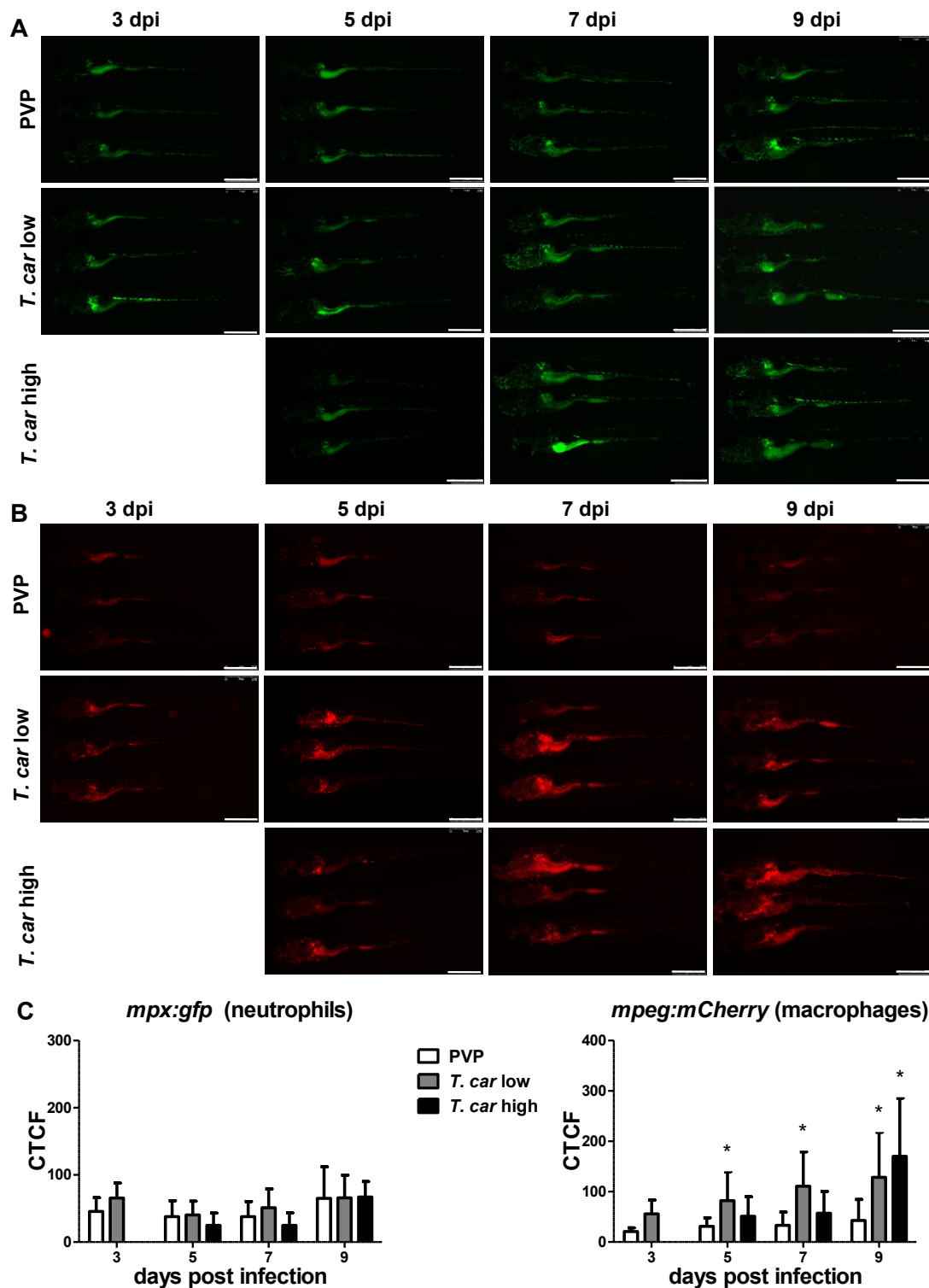
410
411 **Fig 3. Progression of *T. carassii* infection in zebrafish larvae.**
412 *Tg(mpeg1.4:mCherry-F;mpx:GFP)* 5 dpf zebrafish were injected with $n=200$ *T. carassii* or with
413 PVP and imaged at 2 dpi (A), 5 dpi (B-C), 7 dpi (D-E) or sampled at various time points after
414 infection (F). Shown are representative images of intersegmental capillaries (ISC) containing
415 various number of *T. carassii* (white arrows) (A-B); extravasated *T. carassii* (only some
416 indicated with white arrows) in the intraperitoneal cavity (C); cardinal caudal vein diameter in
417 PVP (D) or in *T. carassii*-infected larvae (E). Square brackets indicate the diameter of the
418 cardinal caudal vein. Frames are extracted from high-speed videos acquired with a Leica DMI8
419 inverted microscope at a 40x magnification. F) *T. carassii* infection level. High- and low-infected
420 individuals were separated from 4 dpi onwards based on our clinical scoring criteria. At each
421 time point, 3 pools of 3-5 larvae were sampled for subsequent real-time quantitative gene
422 expression analysis. Each data point represents the mean of 3 pools, except for the high-
423 infected group at 10 dpi where only one pool could be made due to low survival. Relative fold
424 change of the *hsp70* was normalised relative to the zebrafish-specific *ef1a* housekeeping gene
425 and expressed relative to the trypanosome-injected group at time point 0h.

Macrophages and neutrophils response to trypanosome infections in zebrafish

426 ***T. carassii* infection induces a strong macrophage response in zebrafish larvae**

427 After having established a method to determine infection levels in each larva, we next
428 investigated whether a differential innate immune response would be mounted in high-
429 and low-infected fish. To this end, using double-transgenic *Tg(mpeg1.4:mCh-F;mpx:GFP)*
430 zebrafish, we first analysed macrophage and neutrophil responses in whole larvae by
431 quantifying total cell fluorescence in high- and low-infected individuals (**Fig 4**). Total
432 neutrophil response (total green fluorescence) was not significantly affected by the
433 infection (**Fig 4A, 4C**). In contrast, the macrophage response (total red fluorescence)
434 increased significantly in infected individuals from 3 dpi onwards, and was most prominent
435 in the head region and along the cardinal caudal vein (**Fig 4B**). In low-infected larvae, a
436 significant increase in red fluorescence was observed already by 5 dpi and remained high
437 up until 9 dpi; in high-infected larvae, despite a marginal but not significant increase at 5
438 and 7 dpi, significant differences were observed at day 9 after infection (**Fig 4C**).
439 Interestingly, no significant differences were observed between high- or low-infected
440 individuals, suggesting that despite the differences in trypanosome levels (**Fig 3F**),
441 macrophages respond to the presence and not to the number of trypanosomes.

Macrophages and neutrophils response to trypanosome infections in zebrafish



442

443 **Fig 4. Macrophages respond more prominently than neutrophils to *T. carassii***
 444 **infection.** *Tg(mpeg1.4:mCherry-F;mpx:GFP)* were injected intravenously at 5 dpf with $n=200$
 445 *T. carassii* or with PVP. At 4 dpi larvae were separated in high- and low-infected individuals. **A-**
 446 **B)** At the indicated time points, images were acquired with Leica M205FA Fluorescence Stereo
 447 Microscope with 1.79x zoom. Images are representatives of $n=3-44$ larvae per group,
 448 depending on the number of high- or low-infected larvae categorized at each time point. Scale
 449 bar indicates 750 μm . **C)** Corrected Total Cell Fluorescence (CTCF) quantification of infected
 450 and non-infected larvae. Owing to the high auto-fluorescence, the gut area was excluded
 451 from the total fluorescence signal as described in the methods section. Bars represent
 452 average and standard deviation of red and green fluorescence in $n=5-44$ whole larvae, from 2
 453 independent experiments. * indicates significant differences ($P < 0.05$) to the respective PVP
 454 control as assessed by Two-Way ANOVA followed by Bonferroni post-hoc test.

455 ***T. carassii* infection promotes macrophage and neutrophil proliferation**

456 The increase in overall red fluorescence can be indicative of activation of the *mpeg*
457 promotor driving mCherry expression, but also of macrophage proliferation. To address
458 the latter hypothesis, *Tg(mpeg1:eGFP)* or *Tg(mpx:GFP)* zebrafish larvae were infected with
459 *T. carassii*, and subsequently injected with iCLICK™ EdU for identification of proliferating
460 cells. With respect to proliferation, developing larvae display a generalized high rate of cell
461 division throughout the body that increases overtime particularly in hematopoietic organs
462 such as the thymus or the head kidney. Thus, for a more sensitive quantification of the
463 proliferative response of macrophages and neutrophils in response to the infection, EdU
464 was injected at 3 dpi (8 dpf), and at 4 dpi, larvae were separated in high- and low-infected
465 individuals, followed by fixation and whole mount immunohistochemistry 6-8h later (30-
466 32h after EdU injection). This allowed evaluating the macrophage and neutrophil response
467 right at the onset of the macrophage response observed in **Fig 4C** and concomitantly with
468 the development of differences in parasitaemia. As expected, EdU⁺ nuclei could be
469 identified throughout the body of developing larvae. When specifically looking at
470 proliferating macrophage (**Fig 5**) and neutrophils (**Fig 6**) we selected the area of the head
471 (left panels) and trunk (right panels) region, where previously (**Fig 4B**) the highest
472 increase in red fluorescence was observed.

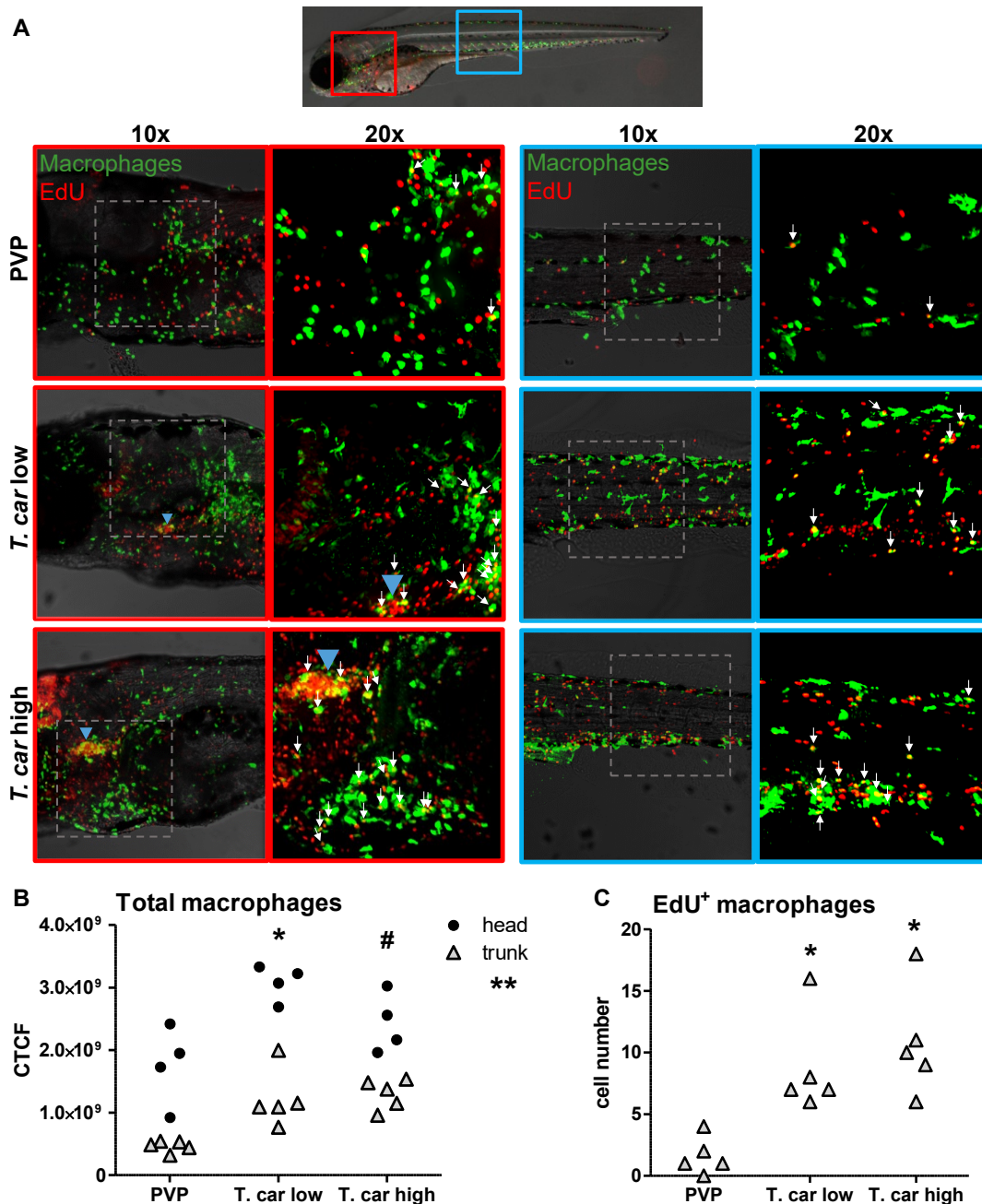
473 When analysing the macrophage response, a greater number of macrophages was
474 observed in the head and trunk of both high- and low-infected larvae compared to PVP-
475 injected individuals (**Fig 5A**, 10x magnifications). In the head, macrophages were
476 scattered throughout the region but in infected larvae they were most abundant in the area
477 corresponding to the haematopoietic tissue (head kidney), posterior to the branchial
478 arches, indicative of proliferation of progenitor cells. In the trunk, macrophages were
479 scattered throughout the tissue, and in high-infected larvae in particular, macrophages
480 also clustered in the cardinal caudal vein (**Fig 5A**, right panels). In agreement with
481 previous observations (**Fig 4C**), quantification of total green fluorescence confirmed a
482 significant increase in the head and trunk of low-infected larvae. In high-infected
483 individuals, a significant increase was observed in the trunk, whereas in the head the
484 number of macrophages was clearly elevated although not significantly when compared to
485 the PVP-injected controls (**Fig 5B**). In all groups, total cell fluorescence in the head region
486 was significantly higher than in the trunk region (**Fig 5B**), and thus largely contributed to
487 the total cell fluorescence previously measured in whole larvae (**Fig 4C**). The difference in
488 CTCF values between Fig 4 and Fig 5 can be attributed to the different microscopes and
489 magnification used for the acquisition as well as fluorescence source (GFP or mCherry in
490 Fig 4 and Alexa-488 fluorophore in Fig 5).

491 Given the high number of macrophages in the head region, their heterogeneous
492 morphology, the thickness of the tissue and the overall high number of EdU⁺ nuclei, it was

Macrophages and neutrophils response to trypanosome infections in zebrafish

493 not possible to reliably count single (EdU⁺) macrophages in this area. Therefore, when
494 analysing the degree of proliferation, we focused on the trunk region only. There, EdU⁺
495 macrophages could be observed in all groups, and in agreement with the total cell
496 fluorescence measured in the same region (**Fig 5B**), their number was higher in low- and
497 high-infected individuals compared to PVP-injected controls (**Fig 5C** and corresponding **S2**
498 **Video**). No significant difference was observed between high- and low-infected fish,
499 confirming that macrophages react to the presence and not to the number of
500 trypanosomes. Within the trunk region of high-infected larvae, a large proportion of
501 macrophages were observed around and inside the cardinal caudal vein, the majority of
502 which were EdU⁺ (**S1A Fig**), suggesting that in high-infected larvae, proliferating
503 macrophages migrated to the vessels. Altogether, these data confirm that *T. carassii*
504 infection triggers macrophage proliferation and that proliferation is higher in low-infected
505 compared to high-infected individuals, possibly due to a higher haematopoietic activity.
506 When analysing the neutrophils response, in agreement with the previous observation, the
507 number of neutrophils in the head and trunk regions was not apparently different between
508 infected and non-infected larvae (**Fig 6A**). Neutrophils were scattered throughout the head
509 region, but differently from macrophages, their number did not increase in the area
510 corresponding to the haematopoietic tissue. Quantification of total cell fluorescence in the
511 head and trunk revealed no significant differences between groups (**Fig 6B**, **S3 Video**).
512 Interestingly, quantification of EdU⁺ neutrophils in the trunk region, revealed that while in
513 PVP-injected individuals EdU⁺ neutrophils were rarely observed, in infected fish, a
514 significant, although low number of EdU⁺ neutrophils was present (**Fig 6C**). These data
515 indicate that neutrophils also respond to the infection by proliferating, but their number is
516 relatively low and may have not significantly contributed to changes in total cell
517 fluorescence. In contrast to macrophages, within the analysed trunk region, neutrophils
518 were never observed within the cardinal caudal vein, and independently of whether they
519 proliferated (EdU⁺) or not, were mostly observed lining the vessel (**S1B Fig**). Altogether,
520 these data indicate that independent of the trypanosome number, *T. carassii* triggers a
521 differential macrophage and neutrophil proliferation, where macrophages respond more
522 prominently than neutrophils to the infection.
523

Macrophages and neutrophils response to trypanosome infections in zebrafish



524

525

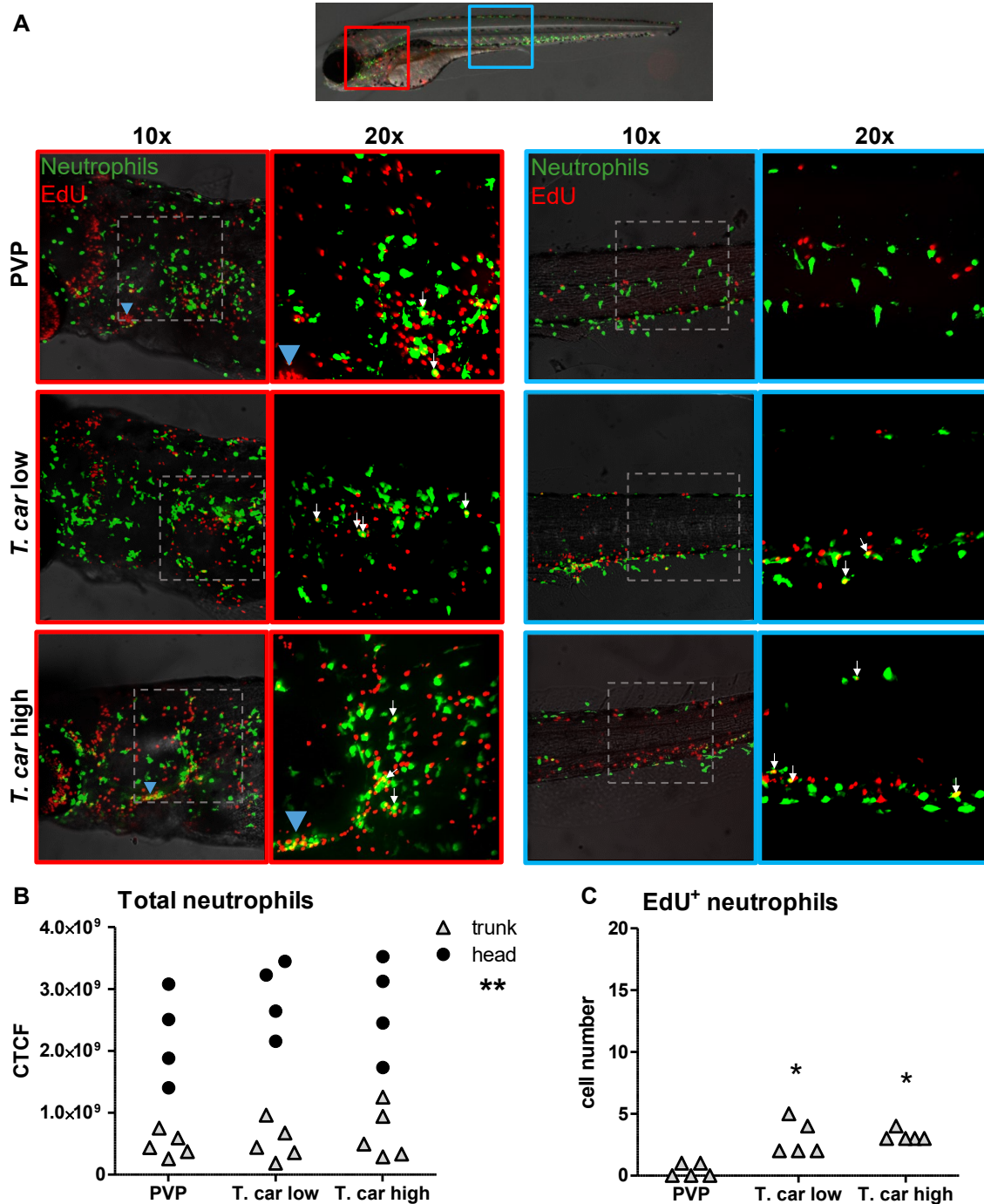
Fig 5. *T. carassii* infection triggers macrophage proliferation.

526 *Tg(mpeg1:eGFP)* zebrafish larvae were infected intravenously at 5 dpf with n=200 *T. carassii*
 527 or with PVP control (n=5 larvae per group, from four independent experiments). At 3 dpi, larvae
 528 received 2 nl 1.13mM iCLICK™ EdU, at 4 dpi were separated in high- and low-infected
 529 individuals and were imaged after fixation and whole mount immunohistochemistry 6-8h later
 530 (30-32h after EdU injection, ~9 dpf). Larvae were fixed and treated with iCLICK EdU ANDY
 531 FLUOR 555 (Red) development to identify EdU⁺ nuclei and with anti-GFP antibody to retrieve
 532 the position of macrophages, as described in the material and methods section. Larvae were
 533 imaged with Andor Spinning Disc Confocal Microscope using 10x and 20x magnification. **A**
 534 Representative maximum projections of the head (left panels, red boxes) and trunk (right
 535 panels, blue boxes) regions capturing macrophages (green) and EdU⁺ nuclei (red) in PVP
 536 control, low- and high-infected zebrafish. In the PVP control group, EdU⁺ nuclei and GFP⁺
 537 macrophages only rarely overlapped (white arrows, 20x), indicating limited proliferation of
 538 macrophages. In high- and low-infected individuals, the number of EdU⁺ macrophages
 539 increased (white arrows, 20x), indicating proliferation of macrophages in response to *T. carassii*
 540 infection. Blue arrowhead in the head of low and high-infected larvae, indicates the position of
 541 the thymus, an actively proliferating organ at this time point. The identification of EdU⁺
 542 macrophages (white arrows) was performed upon detailed analysis of the separate stacks used

Macrophages and neutrophils response to trypanosome infections in zebrafish

543 to generate the overlay images, and are provided in **S2 Video. B)** Corrected total cell
544 fluorescence (CTCF) calculated in the head (circles) and trunk (triangles) region. Symbols
545 indicate individual larvae. * indicates significant differences of both, the head and trunk region
546 to the respective PVP controls; # indicates significant differences of the trunk to the respective
547 PVP control; ** indicates significant differences between CTCF in the head and trunk regions,
548 as assessed by Two-Way ANOVA followed by Bonferroni post-hoc test. **C)** Number of EdU⁺
549 macrophages in the trunk region of infected and non-infected larvae. Symbols indicate
550 individual larvae. * indicates significant differences to the PVP control as assessed by One-Way
551 ANOVA followed by Bonferroni post-hoc test.

Macrophages and neutrophils response to trypanosome infections in zebrafish



552
553
554
555
556
557
558
559
560
561
562
563
564
565
566
567
568

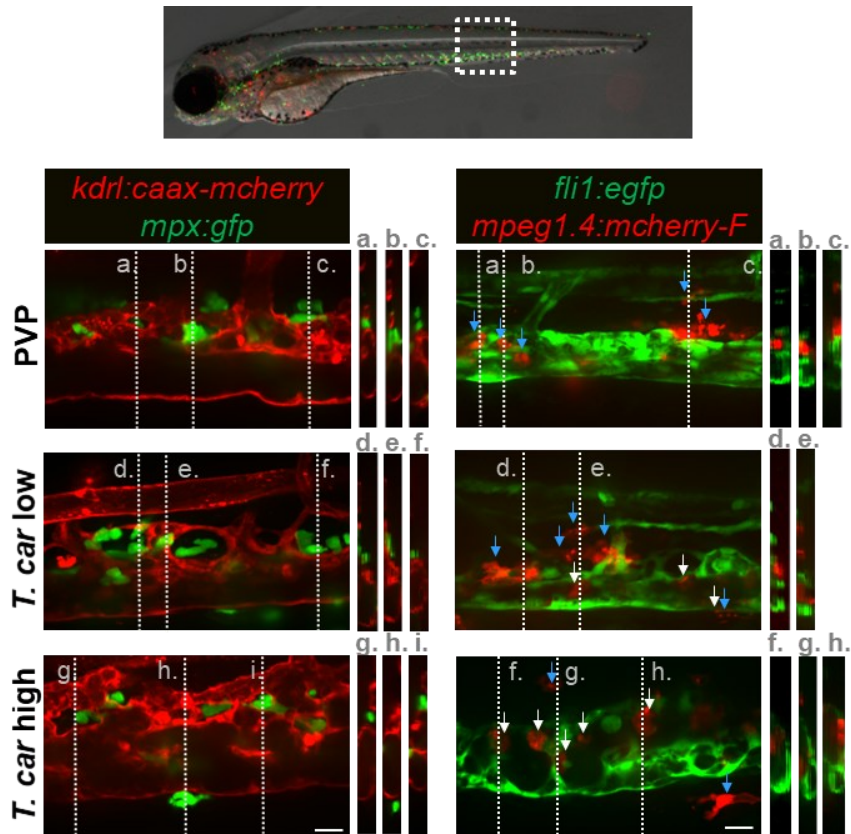
Fig 6. *T. carassii* infection triggers neutrophil proliferation.

Tg(mpx:GFP) were treated as described in Fig 5 (n=5 larvae per group, from four independent experiments). **A**) Representative maximum projections of the head (left panels, red boxes) and trunk (right panels, blue boxes) region capturing neutrophils (green) and EdU⁺ nuclei (red) in PVP, low- and high-infected zebrafish. The images acquired at a 20x magnification show that in all groups, EdU⁺ nuclei and GFP⁺ neutrophils only rarely overlapped (white arrows), and was marginally higher in infected than in non-infected PVP controls. Detailed analysis of the separate stacks selected to compose the overlay image of the head region of the high-infected larva (bottom left panel), revealed that none of the neutrophils in the area indicated by the blue arrowhead (thymus) were EdU⁺ (**S3 Video**). **B**) Corrected total cell fluorescence (CTCF) calculated in the head (circles) and trunk (triangles) region. Symbols indicate individual larvae. ** indicates significant differences between CTCF in the head and trunk regions, as assessed by Two-Way ANOVA followed by Bonferroni post-hoc test. **C**) Number of EdU⁺ neutrophils in the trunk region of infected and non-infected larvae. Symbols indicate individual larvae. * indicates significant differences to the PVP control as assessed by One-Way ANOVA followed by Bonferroni post-hoc test.

569 **Differential distribution of neutrophils and macrophages in high- and low-**
570 **infected zebrafish larvae**

571 After having established that *T. carassii* infection triggers macrophage, and to a lesser
572 extent, neutrophil proliferation, we next investigated whether a differential distribution of
573 these cells occurred during infection. Considering that trypanosomes are blood dwelling
574 parasites and the kinetics of parasitaemia, we focused on the cardinal caudal vein at 4 dpi,
575 a time point at which clear differences in parasitaemia (**Fig 3**) and a differential distribution
576 of macrophages and neutrophils (**Fig 5-6** and **S1 Fig**) were observed between high- and
577 low-infected larvae. To this end, crosses between transgenic lines marking the blood
578 vessels and those marking either macrophages or neutrophils were used. *Tg(kdrl:caax-*
579 *mCherry;mpx:GFP)* or *Tg(fli1:eGFP x mpeg1.4:mCherry-F)* were infected with *T. carassii*,
580 separated into high- and low-infected larvae at 4 dpi, and imaged with Roper Spinning Disk
581 Confocal Microscope using 40x magnification. Longitudinal and orthogonal images of the
582 vessel were analysed to visualise the exact location of cells along the cardinal caudal vein
583 (**Fig 7** and **S4 Video**). In PVP controls, both macrophages and neutrophils were exclusively
584 located outside the vessel in close contact with the endothelium or in the tissue adjacent
585 the cardinal caudal vein. In infected fish, while neutrophils remained exclusively outside
586 the vessel (**Fig 7**, left panel), macrophages could be seen both inside (white arrows) and
587 outside (blue arrows) the vessel (**Fig 7**, right panel). Whilst in low-infected individuals
588 macrophage morphology was similar to that observed in non-infected fish, in high-infected
589 larvae, macrophages inside the vessel clearly had a more rounded morphology. Altogether
590 these data indicate that differently from neutrophils, macrophages increase in number in
591 infected fish, are recruited inside the cardinal caudal vein and, depending on the infection
592 level, their morphology can be greatly affected.

Macrophages and neutrophils response to trypanosome infections in zebrafish



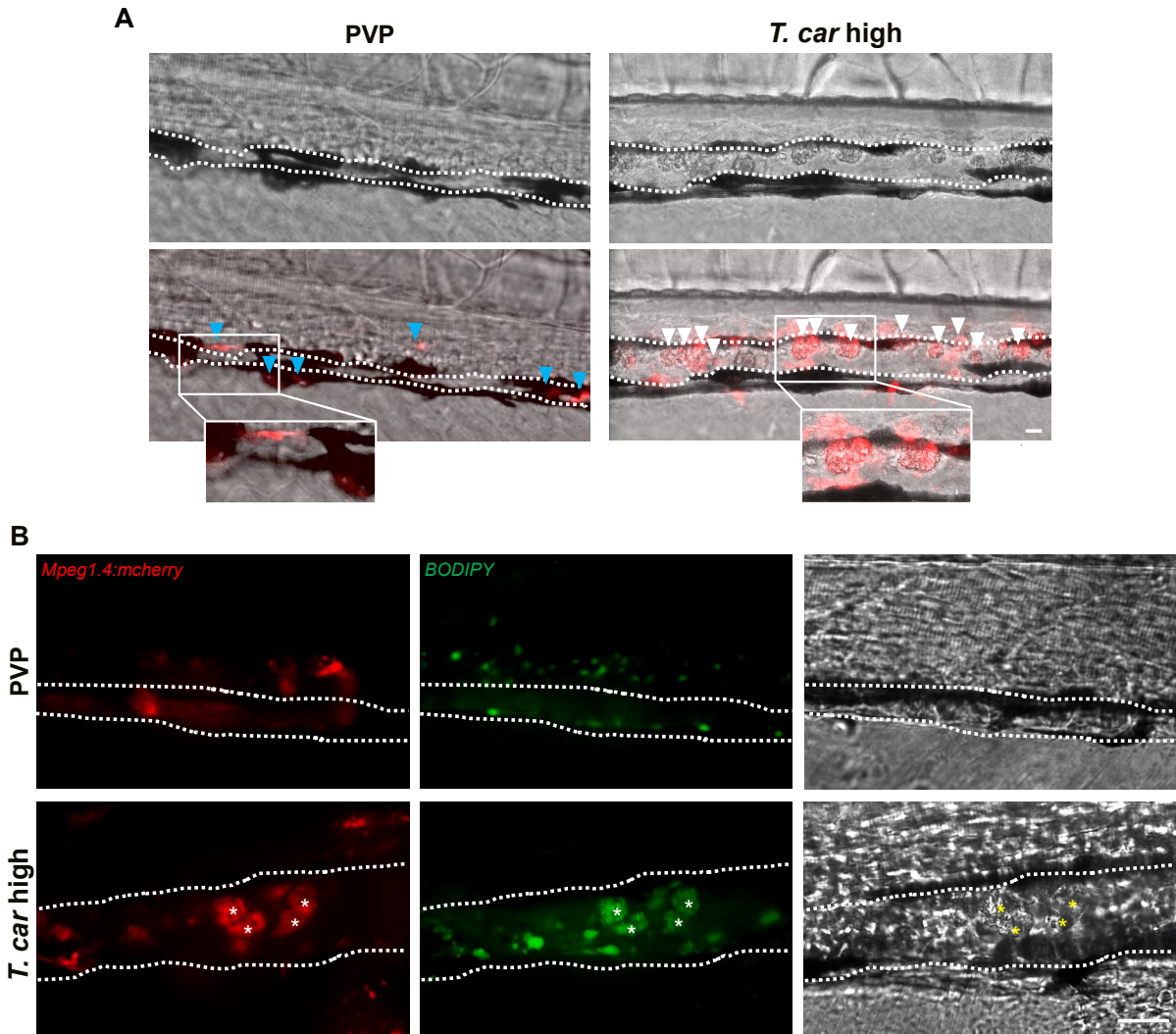
593 **Fig 7. Macrophages are recruited into the cardinal caudal vein of high-infected zebrafish**
594 **larvae.** *Tg(kdr1:caax-mCherry;mpx:GFP)* and *Tg(fli1:eGFP x mpeg1.4: mCherry-F)* zebrafish larvae
595 ($n=5$ larvae per group, from two independent experiments) were injected intravenously at 5 dpf with
596 $n=200$ *T. carassii* or with PVP. At 4 dpi larvae were separated in high- and low-infected groups and
597 imaged with a Roper Spinning Disk Confocal Microscope using 40x magnification. Scale bars indicate
598 25 μm. **Left panel:** representative images of the longitudinal view of the cardinal caudal vein (red),
599 capturing the location of neutrophils (green). Orthogonal views of the locations marked with grey
600 dashed lines (a,b,c,d,e,f,g,h,i), confirm that in all groups, neutrophils are present exclusively outside
601 the vessel. **Right panel:** representative images of the longitudinal view on the vessel, capturing the
602 position of macrophages (red) outside (blue arrowheads) or inside (white arrowheads) the vessel
603 (green). Orthogonal views of the locations marked with grey dashed lines (a,b,c,d,e,f,g,h)
604 confirm that in PVP controls, macrophages are present exclusively outside the vessel (blue arrows); in low-
605 infected larvae, most macrophages are outside the vessel (blue arrows) having an elongated or
606 dendritic morphology, although seldomly rounded macrophages can be observed within the vessel
607 (white arrows); in high-infected larvae, although macrophages with dendritic morphology can be
608 seen outside the vessel, the majority of the macrophages resides inside the vessel, clearly having a
609 rounded morphology. **S4 Video** provides the stacks used for the orthogonal views.

610 ***T. carassii* infection triggers the formation of foamy macrophages in high-infected**
611 **fish**

612 When analysing macrophage morphology and location, clear differences could be observed
613 between control and high- or low-infected larvae when examined in greater detail. In
614 control fish, macrophages generally exhibited an elongated and dendritic morphology,
615 were very rarely observed inside the vessel and were mostly located along the vessel
616 endothelium, in the tissue lining the cardinal vessels or in the ventral fin (**Fig 8A**, left). A
617 similar morphology and distribution were observed in low-infected larvae (not shown).
618 Strikingly, in high-infected larvae, we consistently observed large, dark, granular and
619 round macrophages located almost exclusively inside the cardinal vein on the dorsal
620 luminal side. These dark macrophages were clearly visible already in bright field images
621 due to their size, colour and location, and could be present as single cells or as aggregates
622 (**Fig 8A**, right). The occurrence of these large macrophages increased with the progression
623 of the infection and were exclusive to high-infected individuals (**S5 Video**) as were never
624 observed in low-infected or control larvae.

625 The rounded morphology, size and dark appearance of these cells was reminiscent of that
626 of foamy macrophages. Therefore, to further investigate the nature of these cells, the
627 green fluorescent fatty acid BODIPY-FLC5 was used to track lipid accumulation in infected
628 larvae (**Fig 8B**). Interestingly, administration of BODIPY-FL5 in high-infected larvae, one
629 day prior to the expected appearance of the large macrophages, revealed the accumulation
630 of lipids in these cells (**S6 Video**). Macrophages without this large, dark, granular
631 appearance did not show lipid accumulation. This result therefore confirms that the large,
632 rounded, granular macrophages in the cardinal caudal vein are indeed foamy
633 macrophages.

Macrophages and neutrophils response to trypanosome infections in zebrafish



634

635

636

637

638

639

640

641

642

643

644

645

Fig 8. The large macrophages inside the cardinal caudal vein of high-infected zebrafish are foamy macrophages. A) *Tg(mpeg1.4:mCherry-F; mpx:GFP)* zebrafish larvae were infected intravenously at 5 dpf with $n=200$ *T. carassii* or with PVP ($n=5$ larvae per group) and imaged at 7 dpi using an Andor Spinning Disc Confocal Microscope at a 20x magnification. Representative images from three independent experiments are shown, with blue arrowheads pointing at macrophages outside the vessel and white arrowheads indicating large round macrophages inside the cardinal vein (dashed line). Scale bar indicates 25 μm . **B)** *Tg(mpeg1.4:mCherry-F)* were treated as in A ($n=5$ larvae per group). At 3 dpi, larvae received 1 nl of 30 μM BODIPY-FLC5 and were imaged 18-20 hours later using a Roper Spinning Disc Confocal Microscope at a 40x magnification. Representative images from three independent experiments are shown. Scale bar indicates 25 μm . **S6 Video** provides the stacks used in B.

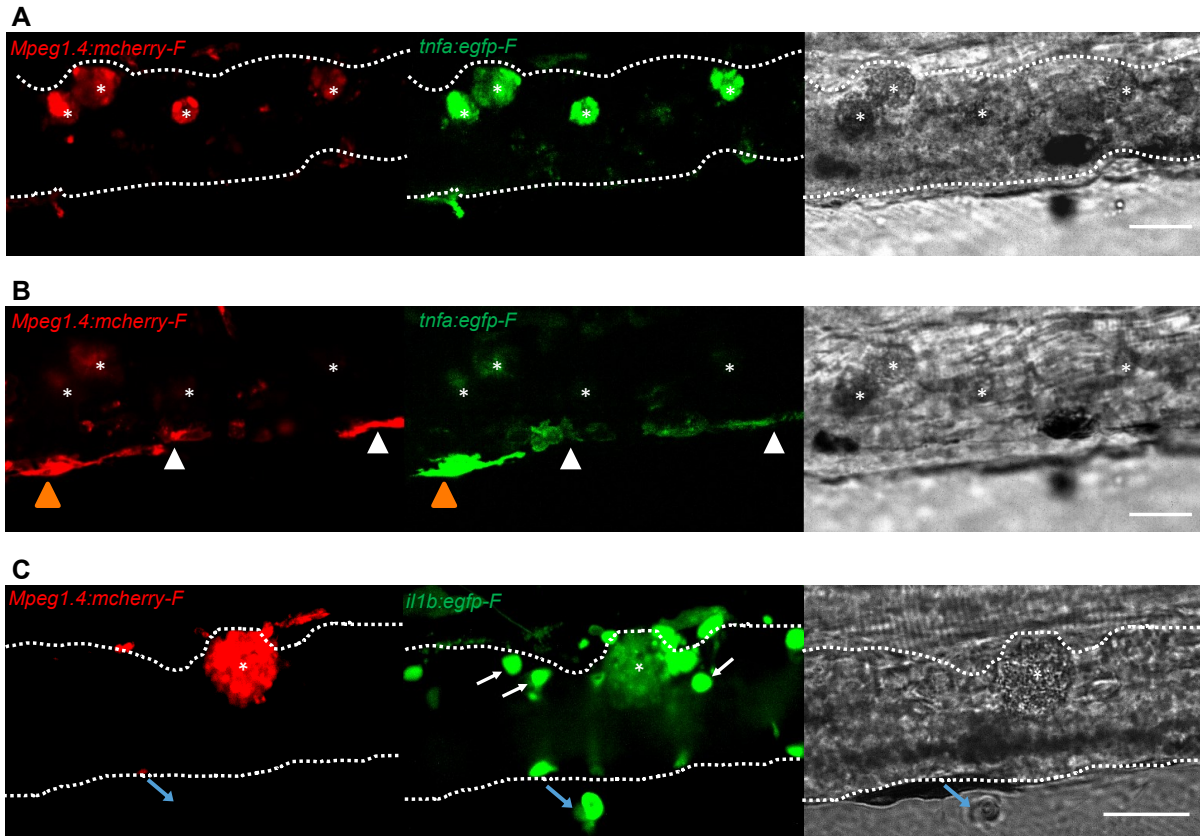
Macrophages and neutrophils response to trypanosome infections in zebrafish

646 **Foamy macrophages have a pro-inflammatory activation state**

647 To further investigate the activation state of foamy macrophages, we made use of the
648 *Tg(tnfa:eGFP-F;mpeg1.4:mCherry-F)* and *Tg(il1b:eGFP-F x mpeg1.4:mCherry-F)* double
649 transgenic zebrafish lines, having macrophages in red and *tnfa*- or *Il1b*-expressing cells in
650 green (**Fig 9** and **Fig 10**). We first focused on the time point at which the foamy
651 macrophages were most clearly present in highly infected individuals, 4 dpi. Our results
652 clearly show that all large foamy macrophages, were strongly positive for *tnfa*, suggesting
653 an inflammatory activation state (**Fig 9A**). Interestingly, not only the large foamy
654 macrophages within the vessel, but also dendritic or lobulated macrophages outside or
655 lining the vessel showed various degrees of activation. Macrophages that were still partly
656 in the vessel (**Fig 9B**, yellow arrowhead) displayed higher *tnfa* expression than
657 macrophages lining the outer endothelium (white arrow heads). This could suggest that
658 the presence of *T. carassii* components within the vessels might trigger macrophage
659 activation.

660 Similar to what observed for *tnfa* expression, all foamy macrophages within the vessel
661 were also positive for *il1b* (**Fig 9C**, asterisk), confirming their pro-inflammatory profile.
662 Interestingly, not only macrophages but also endothelial cells (a selection is indicated by
663 white arrows) were strongly positive for *il1b*. Outside the vessel, cells that were mCherry
664 negative but strongly positive for *Il1b* could also be observed (**Fig 9C**, blue arrow); given
665 their position outside the vessel, these are most likely neutrophils. Altogether these data
666 indicate that foamy macrophages occur in high-infected larvae and have a strong pro-
667 inflammatory profile.

Macrophages and neutrophils response to trypanosome infections in zebrafish



668
669
670
671
672
673
674
675
676
677
678
679
680
681
682

Fig 9. Foamy macrophages have an inflammatory profile.

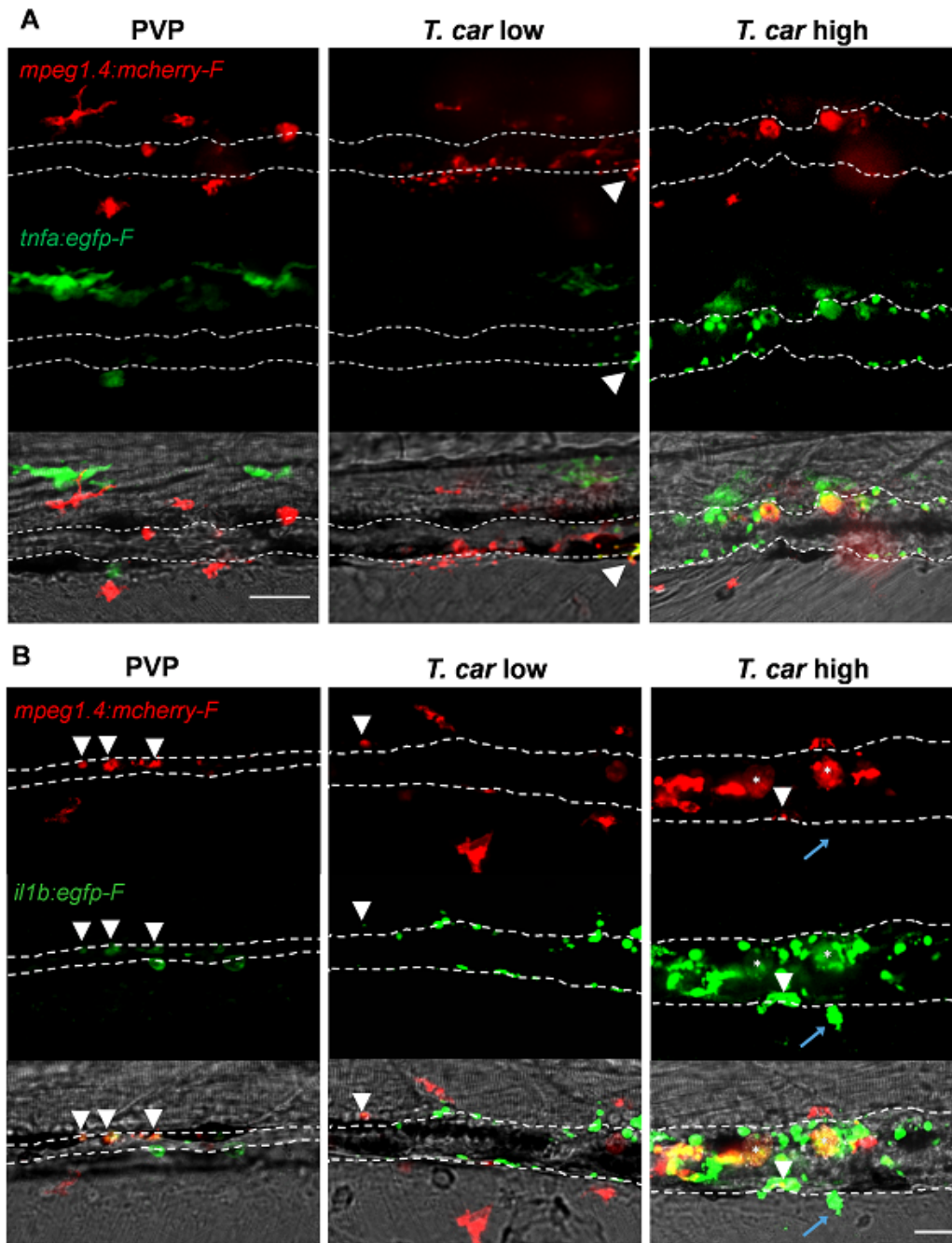
Tg(tnfa:eGFP-F;mpeg1.4:mCherry-F) **A-B** or *Tg(il1b:eGFP-F x mpeg1.4:mcherry-F)* **C** zebrafish larvae (5dpf), were injected with n=200 *T. carassii* or with PVP. At 4 dpi, high-infected individuals were imaged with an Andor **(A-B)** or Roper **(C)** Spinning Disk Confocal Microscope using 40x magnification. Scale bar indicates 25 μm. Foamy macrophages (asterisks) were easily identified within the cardinal caudal vessel (dashed lines) and were strongly positive for *tnfa* **(A)** and *il1b* **(C)** expression (GFP signal). **B** Same as in A, but a few stacks up, focusing on the cells lining the endothelium. Macrophages that were partly inside and partly outside the vessel (yellow arrowhead) were also strongly positive for *tnfa*, whereas macrophages lining the outer endothelium had a lower *tnfa* expression (white arrowheads). **C** A foamy macrophage (asterisk) within the cardinal caudal vessel (dashed lines) was positive for *il1b*. Endothelial cells were also strongly positive for *il1b*, a selection of which is indicated by white arrows. A mCherry-negative-Il1b positive cell is present outside the vessel (blue arrow). Given its position, it is likely to be a neutrophil.

Macrophages and neutrophils response to trypanosome infections in zebrafish

683 **High-infected zebrafish have a strong inflammatory profile associated with**
684 **susceptibility to infection**

685 When comparing the overall inflammatory state in high- and low-infected larvae it was
686 apparent that high-infected individuals generally exhibited a higher pro-inflammatory
687 response (**Fig 10**). Although *tnfa*- and *il1b*-positive macrophages could be seen in low-
688 infected individuals, these were generally few (**Fig 10A** and **10B**, middle panels) and a
689 higher number of *tnfa*- and *il1b*-expressing cells was observed in high-infected larvae (**Fig**
690 **10A** and **10B**, right panels). In these fish, *il1b* and *tnfa* expression was observed not only
691 in (foamy) macrophages (asterisk), but also in mCherry negative cells outside the vessel
692 (blue arrow, likely neutrophils) and in endothelial cells lining the vessel (bright green). As
693 mentioned earlier, high-infected individuals are not able to control parasitaemia and
694 generally succumbed to the infection. Altogether, these results suggest that in high-
695 infected individuals, uncontrolled parasitaemia leads to an exacerbated pro-inflammatory
696 response leading to susceptibility to the infection. Low-infected individuals however, with
697 increased macrophage number and moderate cytokine responses, are able to control
698 parasitaemia and to recover from the infection.

Macrophages and neutrophils response to trypanosome infections in zebrafish



699

700

701

702

703

704

705

706

707

708

709

710

711

712

713

714

715

716

717

Fig 10. High-infected zebrafish have a strong inflammatory profile.

Zebrafish larvae (5 dpf), either (A) *Tg(tnfa:eGFP-F x mpeg1.4:mCherry-F)* (n= 8-13 larvae per group from four independent experiments), or (B) *Tg(il1b:eGFP-F; mpeg1.4:mCherry-F)* (n=7-8 larvae per group from two independent experiments), were infected as described in Fig 7. At 3 dpi, larvae were separated in high- and low-infected individuals and at 4 dpi imaged with a Roper Spinning Disk Confocal Microscope. Scale bar indicate 25 μ m. **A)** In non-infected PVP controls (left panel), several macrophages can be observed outside the vessel but none was positive for *tnfa*. In low-infected individuals (middle panel) macrophages were present inside and outside the vessel. Except the occasional macrophage showing *tnfa-egfp* expression (white arrowhead), they generally did not exhibit strong GFP signal. In high-infected individuals however, foamy macrophages (asterisks) as well as endothelial cells (bright green cells) or other leukocytes, were strongly positive for *tnfa-egfp* expression. **B)** *il1b-egfp* expression was generally low in non-infected PVP controls. In low-infected larvae *il1b* positive macrophages were rarely observed (white arrowhead). In both high- and low-infected fish, some endothelium cells in the cardinal caudal vein show high *il1b-egfp* expression (bright green cells in middle and right panel). In high-infected individual however (right panel), foamy macrophages inside the vessel (asterisks) as well as other macrophages lining the vessel (white arrowhead) and leukocytes in the tissue (blue arrow), were positive for *il1b-egfp* expression.

718 **Discussion**

719

720 In this study we describe the differential response of macrophages and neutrophils *in vivo*,
721 during the early phase of trypanosome infection of larval zebrafish. Considering the
722 prominent role of innate immune factors in determining the balance between pathology
723 and control of first-peak parasitaemia in mammalian models of trypanosomiasis (Magez
724 and Caljon, 2011; Radwanska et al., 2018; Stijlemans et al., 2017), the use of transparent
725 zebrafish larvae, devoid of a fully developed adaptive immune system, allowed us to
726 investigate the early events of the innate immune response to *T. carassii* infection *in vivo*.
727 After having established a clinical scoring system of infected larvae, we were able to
728 consistently differentiate high- and low-infected individuals, each associated with opposing
729 susceptibility to the infection. In high-infected larvae, which fail to control first-peak
730 parasitaemia, we observed a strong inflammatory response associated with the occurrence
731 of foamy macrophages and susceptibility to the infection. Conversely, in low-infected
732 individuals, which succeeded in controlling parasitaemia, we observed a moderate
733 inflammatory response associated with resistance to the infection. Altogether these data
734 confirm that also during trypanosome infection of zebrafish, innate immunity is sufficient
735 to control first-peak parasitaemia and that a controlled inflammatory response is beneficial
736 to the host.

737 Using transgenic lines marking macrophages and neutrophils, total cell fluorescence and
738 cell proliferation analysis revealed that *T. carassii* infection triggers macrophage
739 proliferation, particularly in low-infected individuals. Although to a much lesser extent,
740 neutrophils also responded to the infection by proliferating. The total number of neutrophils
741 however, was comparatively low and likely did not contribute to the total cell fluorescence
742 measured in our whole larvae analysis. Although neutrophils were recently implicated in
743 promoting the onset of tsetse fly-mediated trypanosome infections in mouse dermis,
744 macrophage-derived immune mediators, such as NO and TNF α were confirmed to played
745 a more prominent role in the control of first-peak parasitaemia and in the regulation of the
746 overall inflammatory response (Caljon et al., 2018).

747 The observation that in low-infected individuals the number of macrophages was
748 significantly increased by 4-5 dpi, the time point at which clear differences in parasitaemia
749 were apparent between the two infected groups, suggests a role for macrophages, or for
750 macrophage-derived factors in first-peak parasitaemia control. Phagocytosis however, can
751 be excluded as one of the possible contributing factors since motile *T. carassii*, similar to
752 other extracellular trypanosomes (Caljon et al., 2018; Saeij et al., 2003; Scharsack et al.,
753 2003), cannot be engulfed by any innate immune cell. A strong inflammatory response is
754 also not required for trypanosomes control, since in low-infected individuals, only moderate
755 *il1b* or *tnfa* expression was observed, mostly in macrophages, as assessed using transgenic

Macrophages and neutrophils response to trypanosome infections in zebrafish

756 zebrafish reporter lines. Our data are in agreement with several previous studies using
757 trypanoresistant (BALB/c) or trypanosusceptible (C57Bl/6) mice that revealed the double-
758 edge sword of pro-inflammatory mediators such as TNF α or IFN γ during trypanosome
759 infection in mammalian models (reviewed by Radwanska et al., 2018; Stijlemans et al.,
760 2007). These studies showed that a timely but controlled expression of IFN γ , TNF α and
761 NO, contributed to trypanosomes control via direct (Daulouede et al., 2001; F Iraqi et al.,
762 2001; Lucas et al., 1994) or indirect mechanisms (Kaushik et al., 1999; Magez et al., 2007,
763 2006; Mansfield and Paulnock, 2005; Namangala et al., 2001; Noël et al., 2002).
764 Conversely, in individuals in which an uncontrolled inflammatory response took place,
765 immunosuppression and inflammation-related pathology occurred (Namangala et al.,
766 2009, 2001; Noël et al., 2004; Stijlemans et al., 2016). The stark contrast between the
767 mild inflammatory response observed in low-infected individuals and the exacerbated
768 response observed in high-infected larvae, strongly resembles the opposing responses
769 generally observed in trypanoresistant or trypanosusceptible animal models. Owing to the
770 possibility to monitor the infection at the individual level, it was possible to observe such
771 responses within one population of outbred zebrafish larvae. Although we were unable to
772 investigate the specific role of *Tnfa* during *T. carassii* infection of zebrafish, due to the
773 unavailability of *tnfa*^{-/-} zebrafish lines or the unsuitability of morpholinos for transient
774 knock-down at late stages of development, we previously reported that recombinant
775 zebrafish (as well as carp and trout) *Tnfa*, are all able to directly lyse *T. brucei* (Forlenza
776 et al., 2009). In the same study, we reported that also during *Trypanoplasma borreli*
777 (kinetoplastid) infection of common carp, soluble as well as transmembrane carp *Tnfa* play
778 a crucial role in both trypanosome control and susceptibility to the infection. Thus,
779 considering the evolutionary conservation of the lectin-like activity among vertebrate's
780 TNF α (Daulouede et al., 2001; Forlenza et al., 2009; R Lucas et al., 1994; Magez et al.,
781 1997) it is possible that the direct lytic activity of zebrafish *Tnfa* may have played a role in
782 the control of first-peak parasitaemia in low-infected individuals. In the future, using *tnfa*^{-/-}
783 zebrafish lines, possibly in combination with *ifn γ* reporter or *ifn γ* ^{-/-} lines, it will be
784 possible to investigate in detail the relative contribution of these inflammatory mediators
785 in the control of parasitaemia as well as onset of inflammation.

786 There are multiple potential explanations for the inability of high-infected larvae to control
787 parasitaemia and the overt inflammatory response. Using various comparative mice
788 infection models, it became apparent that while TNF α production is required for
789 parasitaemia control, a timely shedding of TNF α Receptor-2 (TNFR2) is necessary to limit
790 TNF α -mediated infection-associated immunopathology (Radwanska et al., 2018).
791 Furthermore, during *T. brucei* infection in mice and cattle, continuous cleavage of
792 membrane Glycosyl-phosphatidyl-inisitol (GPI)-anchored VSG (mVSG-GPI) leads to
793 shedding of the soluble VSG-GIP (sVSG-GPI), while the di-myristoyl-glycerol compound

Macrophages and neutrophils response to trypanosome infections in zebrafish

794 (DMG) is left in the membrane. While the galactose-residues of sVSG-GPI constituted the
795 minimal moiety required for optimal TNF α production, the DMG compound of mVSG
796 contributed to macrophage overactivation (TNF α and IL-1 β secretion) (Magez et al., 2002,
797 1998; Sileghem et al., 2001). Although *T. carassii* was shown to possess a surface
798 dominated by GPI-anchored carbohydrate-rich mucin-like glycoproteins, not subject to
799 antigenic variation (LISCHKE et al., 2000; Overath et al., 2001), components of its
800 excreted/secreted proteome, together with phospholipase C-cleaved GPI-anchored surface
801 proteins, have all been shown to play a role in immunogenicity (Joerink et al., 2007),
802 inflammation (Oladiran and Belosevic, 2010, 2009; Ribeiro et al., 2010) as well as
803 immunosuppression (Oladiran and Belosevic, 2012). Thus, the overactivation caused by
804 the presence of elevated levels of pro-inflammatory trypanosome-derived moieties,
805 combined with the lack of a timely secretion of regulatory molecules (e.g. soluble TNFR2)
806 that could control the host response, may have all contributed to the exacerbated
807 inflammation observed in high-infected individuals.

808 Given the differential response observed in low- and high-infected individuals, especially
809 with respect to macrophage distribution and activation, we attempted to investigate the
810 specific role of macrophages in the protection or susceptibility to *T. carassii* infection. To
811 this end, the use of a cross between the *Tg(mpeg1:Gal4FF)^{g12}* (Ellett et al., 2011) and the
812 *Tg(UAS-E1b:Eco.NfsB-mCherry)^{c26}* (Davison et al., 2007) line, which would have allowed
813 the timed metronidazole (MTZ)-mediated depletion of macrophages in zebrafish larvae,
814 was considered. Unfortunately, *in vitro* analysis of the effect of MTZ on the trypanosome
815 itself, revealed that trypanosomes are susceptible to MTZ, rendering the *nfsB* line not
816 suitable to investigate the role of macrophages (nor neutrophils) during this particular type
817 of infection. Alternatively, we attempted to administer liposome-encapsulated clodronate
818 (Lipo-clodronate) as described previously (Nguyen-Chi et al., 2017; Phan et al., 2018;
819 Travnickova et al., 2015). In our hands however, administration of 5 mg/ml Lipo-
820 clodronate (3 nl) to 5 dpf larvae (instead of 2-3 dpf larvae), led to the rapid development
821 of oedema.

822 Besides differences between the overall macrophage and neutrophil (inflammatory)
823 response, the differential distribution of these cells was also investigated *in vivo* during
824 infection utilising the transparency of the zebrafish and the availability of transgenic lines
825 marking the vasculature. Neutrophils were never observed inside the cardinal caudal vein
826 although in infected individuals they were certainly recruited and were observed in close
827 contact with the outer vessel's endothelium. Conversely, macrophages could be seen both
828 outside and inside the vessel and the total proportion differed between high- and low-
829 infected individuals. While in low-infected individuals the majority of macrophages
830 recruited to the cardinal caudal vein remained outside the vessel in close contact with the
831 endothelium, in high-infected individuals the majority of macrophages were recruited

Macrophages and neutrophils response to trypanosome infections in zebrafish

832 inside the caudal vein and were tightly attached to the luminal vessel wall. To our
833 knowledge, such detailed description of the relative (re)distribution of neutrophils and
834 macrophages, *in vivo*, during a trypanosome infection, has not been reported before.
835 Interestingly, exclusively in high-infected individuals, by 4 dpi large, round, dark and
836 granular cells were observed, already under the bright field view, in the lumen of the
837 cardinal caudal vein. These cells were confirmed to be foamy macrophages with high
838 cytoplasmic lipid content. Foam cells, or foamy macrophages have been named after the
839 lipid bodies accumulated in their cytoplasm leading to their typical enlarged morphological
840 appearance (Dvorak et al., 1983), but are also distinguished by the presence of diverse
841 cytoplasmic organelles (Melo et al., 2003). They have been associated with several
842 (intracellular) infectious diseases, including Leishmaniasis, Chagas disease, experimental
843 malaria, toxoplasmosis and tuberculosis, (reviewed in (López-Muñoz et al., 2018; Vallochi
844 et al., 2018)) but never before with (extracellular) trypanosome infection. For example,
845 during *T. cruzi* infection of rat, increased numbers of activated monocytes or macrophages
846 were reported in the blood or heart (Melo and Machado, 2001). Interestingly, trypanosome
847 uptake was shown to directly initiate the formation of lipid bodies in macrophages, leading
848 to the appearance of foamy macrophages (D'Avila et al., 2011). During human
849 *Mycobacterium tuberculosis* infections, foamy macrophages play a role in sustaining the
850 presence of bacteria and contribute to tissue cavitation enabling the spread of the infection
851 (Russell et al., 2009). Independently of the disease, it is clear that foamy macrophages
852 are generally associated with inflammation, since their cytoplasmic lipid bodies are a source
853 of eicosanoids, strong mediators of inflammation (Melo et al., 2006; Wymann and
854 Schneider, 2008). In turn, inflammatory mediators such as Prostaglandin E2 benefit
855 trypanosome survival, as shown in *Trypanosoma*, *Leishmania*, *Plasmodium*, and
856 *Toxoplasma* infections (reviewed in Vallochi et al., 2018). Our results are consistent with
857 these reports as we show the occurrence of foamy macrophages exclusively in individuals
858 that developed high parasitaemia, characterized by a strong pro-inflammatory response,
859 and ultimately succumbed to the infection. Although we did not systematically investigate
860 the exact kinetics of parasitaemia development in correlation with foamy macrophages
861 occurrence, during our *in vivo* monitoring, we consistently observed that the increase in
862 trypanosome number preceded the appearance of foamy macrophages. It is possible that,
863 in high-infected individuals, foamy macrophages are formed due to the necessity to clear
864 the increasing concentration of circulating trypanosome-derived moieties or of dying
865 trypanosomes. The interaction with trypanosome-derived molecules, including soluble
866 surface (glyco)proteins or trypanosome DNA, may not only be responsible for the activation
867 of pro-inflammatory pathways, but also for a change in cell metabolism. The occurrence of
868 foamy macrophages has been reported for intracellular trypanosomatids (*T. cruzi*,
869 *Leishmania*), and arachidonic acid-derived lipids were reported to act as regulators of the

Macrophages and neutrophils response to trypanosome infections in zebrafish

870 host immune response and trypanosome burden during *T. brucei* infections (López-Muñoz
871 et al., 2018). To our knowledge our study is the first to report the presence of foamy
872 macrophages during an extracellular trypanosome infection.

873 The possibility to detect the occurrence of large, granular cells already in the bright field
874 and the availability of transgenic lines that allowed us to identify these cells as
875 macrophages, further emphasizes the power of the zebrafish model. It allowed us to
876 visualise *in vivo*, in real time, not only their occurrence but also their differential distribution
877 with respect to other macrophages or neutrophils. Observations that we might have missed
878 if we for example were to bleed an animal, perform immunohistochemistry or gene
879 expression analysis. Thus, the possibility to separate high- and low-infected animals
880 without the need to sacrifice them, allowed us to follow at the individual level the
881 progression of the infection and the ensuing differential immune response.

882 In the future it will be interesting to analyse the transcription profiles of sorted macrophage
883 populations from low- and high-infected larvae. Given the marked heterogeneity in
884 macrophage activation observed especially within high-infected individuals, single-cell
885 transcriptome analysis, of foamy macrophages in particular, may provide insights in the
886 differential activation state of the various macrophage phenotypes. Furthermore, the
887 zebrafish has already emerged as a valuable animal model to study inflammation and host-
888 pathogen interaction and can be a powerful complementary tool to examine macrophage
889 plasticity and polarization *in vivo*, by truly reflecting the complex nature of the environment
890 during an ongoing infection in a live host. Finally, the availability of (partly) transparent
891 adult zebrafish lines (Antinucci and Hindges, 2016; White et al., 2008), may aid the *in vivo*
892 analysis of macrophage activation in adult individuals.

893 Altogether, in this study we describe the innate immune response of zebrafish larvae to *T.*
894 *carassii* infection. The transparency and availability of various transgenic zebrafish lines,
895 enabled us to establish a clinical scoring system that allowed us to monitor parasitaemia
896 development and describe the differential response of neutrophils and macrophages at the
897 individual level. Interestingly, for the first time in an extracellular trypanosome infection,
898 we report the occurrence of foamy macrophages, characterized by a high lipid content and
899 strong inflammatory profile, associated with susceptibility to the infection. Our model paves
900 the way to investigate which mediators of the trypanosomes are responsible for the
901 induction of such inflammatory response as well as study the condition that lead to the
902 formation of foamy macrophages *in vivo*.

903

904 **Acknowledgments**

905 This work was supported by the FishForPharma FP7 People: Marie Curie Initial Training
906 Network, project number PITN-GA-2011-289209 and by the Dutch Research Council
907 (NWO), project number 022.004.005. Dr. Christelle Langevin from Institut National de la

Macrophages and neutrophils response to trypanosome infections in zebrafish

908 Recherche Agronomique (INRA) is greatly acknowledged for her assistance with
909 immunohistochemical analysis. The authors like to thank Dr. Danilo Pietretti, Marleen
910 Scheer, and Dr. Sylvia Brugman from the Cell Biology and Immunology Group of
911 Wageningen University & Research (WUR) for technical support with the RQ-PCR analysis,
912 parasite isolation and for fruitful discussions; the CARUS Aquatic Research Facility of WUR
913 is acknowledged for fish rearing and husbandry. Prof. Mark Carrington, Cambridge
914 University, is acknowledged for the fruitful discussions and for revising the manuscript.
915 Furthermore, the authors like to thank Dr. Norbert de Ruijter from the Wageningen Light
916 Microscopy Centre, and the Montpellier Resources Imagerie facility for their assistance.

917

918 **References**

- 919 Antinucci P, Hindges R. 2016. A crystal-clear zebrafish for in vivo imaging. *Sci Rep* **6**.
920 doi:10.1038/srep29490
- 921 Baral TN, De Baetselier P, Brombacher F, Magez S. 2007. Control of Trypanosoma evansi Infection
922 Is IgM Mediated and Does Not Require a Type I Inflammatory Response. *J Infect Dis*
923 **195**:1513–1520. doi:10.1086/515577
- 924 Benard EL, Racz PI, Rougeot J, Nezhinsky AE, Verbeek FJ, Spaink HP, Meijer AH. 2015.
925 Macrophage-expressed perforins Mpeg1 and Mpeg1.2 have an anti-bacterial function in
926 zebrafish. *J Innate Immun* **7**:136–152. doi:10.1159/000366103
- 927 Bertrand JY, Chi NC, Santoso B, Teng S, Stainier DYR, Traver D. 2010. Haematopoietic stem cells
928 derive directly from aortic endothelium during development. *Nature* **464**:108–111.
929 doi:10.1038/nature08738
- 930 Boada-Sucre AA, Rossi Spadafora MS, Tavares-Marques LM, Finol HJ, Reyna-Bello A. 2016.
931 Trypanosoma vivax Adhesion to Red Blood Cells in Experimentally Infected Sheep. *Patholog*
932 *Res Int* **2016**. doi:10.1155/2016/4503214
- 933 Caljon G, Mabile D, Stijlemans B, Trez C De, Mazzone M, Tacchini-cottier F, Malissen M,
934 Ginderachter JA Van, Magez S, Baetselier P De, Abbeele J Van Den. 2018. Neutrophils
935 enhance early Trypanosoma brucei infection onset 1–11. doi:10.1038/s41598-018-29527-y
- 936 Chi NC, Shaw RM, Val S De, Kang G, Jan LY, Black BL, Stainier DYR. 2008. Expression and
937 Atrioventricular Canal Formation. *Genes Dev* 734–739. doi:10.1101/gad.1629408.734
- 938 Cnops J, De Trez C, Stijlemans B, Keirsse J, Kauffmann F, Barkhuizen M, Keeton R, Boon L,
939 Brombacher F, Magez S. 2015. NK-, NKT- and CD8-Derived IFN γ Drives Myeloid Cell
940 Activation and Erythrophagocytosis, Resulting in Trypanosomosis-Associated Acute Anemia.
941 *PLoS Pathog* **11**. doi:10.1371/journal.ppat.1004964
- 942 Collier SP, Mansfield JM, Paulnock DM. 2003. Glycosylinositolphosphate Soluble Variant Surface
943 Glycoprotein Inhibits IFN- γ -Induced Nitric Oxide Production Via Reduction in STAT1
944 Phosphorylation in African Trypanosomiasis. *J Immunol* **171**:1466–1472.
945 doi:10.4049/jimmunol.171.3.1466
- 946 Cronan MR, Tobin DM. 2014. Fit for consumption: zebrafish as a model for tuberculosis. *Dis Model*
947 *Mech*. doi:10.1242/dmm.016089
- 948 D'Avila H, Freire-de-Lima CG, Roque NR, Teixeira L, Barja-Fidalgo C, Silva AR, Melo RCN, DosReis
949 GA, Castro-Faria-Neto HC, Bozza PT. 2011. Host cell lipid bodies triggered by Trypanosoma
950 cruzi infection and enhanced by the uptake of apoptotic cells are associated with
951 prostaglandin E2 generation and increased parasite growth. *J Infect Dis* **204**:951–961.
952 doi:10.1093/infdis/jir432
- 953 Daulouede S, Bouteille B, Moynet D, De Baetselier P, Courtois P, Lemesre JL, Buguet A, Cespuglio
954 R, Vincendeau P. 2001. Human macrophage tumor necrosis factor (TNF)-alpha production
955 induced by Trypanosoma brucei gambiense and the role of TNF-alpha in parasite control. *J*
956 *Infect Dis* **183**:988–991.
- 957 Davison JM, Akitake CM, Goll MG, Rhee JM, Gosse N, Baier H, Halpern ME, Leach SD, Parsons MJ.
958 2007. Transactivation from Gal4-VP16 transgenic insertions for tissue-specific cell labeling
959 and ablation in zebrafish. *Dev Biol* **304**:811–824. doi:10.1016/j.ydbio.2007.01.033
- 960 Dóro É, Jacobs SH, Hammond FR, Schipper H, Pieters RP, Carrington M, Wiegertjes GF, Forlenza M.
961 2019. Visualizing trypanosomes in a vertebrate host reveals novel swimming behaviours,
962 adaptations and attachment mechanisms. *Elife* **8**. doi:10.7554/elife.48388

Macrophages and neutrophils response to trypanosome infections in zebrafish

- 963 Dvorak AM, Dvorak HF, Peters SP, Shulman ES, MacGlashan DWJ, Pyne K, Harvey VS, Galli SJ,
964 Lichtenstein LM. 1983. Lipid bodies: cytoplasmic organelles important to arachidonate
965 metabolism in macrophages and mast cells. *J Immunol* **131**:2965–2976.
- 966 Ellett F, Pase L, Hayman JW, Andrianopoulos A, Lieschke GJ. 2011. Mpeg1 Promoter Transgenes
967 Direct Macrophage-Lineage Expression in Zebrafish. *Blood* **117**:e49–e56. doi:10.1182/blood-
968 2010-10-314120
- 969 Engstler M, Pfohl T, Herminghaus S, Boshart M, Wiegertjes G, Heddergott N, Overath P. 2007.
970 Hydrodynamic Flow-Mediated Protein Sorting on the Cell Surface of Trypanosomes. *Cell*
971 **131**:505–515. doi:10.1016/j.cell.2007.08.046
- 972 Forlenza M, Kaiser T, Savelkoul HFJ, Wiegertjes GF. 2012. The use of real-time quantitative PCR for
973 the analysis of cytokine mRNA levels. *Methods in Molecular Biology* (Clifton, N.J.). pp. 7–23.
974 doi:10.1007/978-1-61779-439-1_2
- 975 Forlenza M, Magez S, Scharsack JP, Westphal A, Savelkoul HFJ, Wiegertjes GF. 2009. Receptor-
976 Mediated and Lectin-Like Activities of Carp (*Cyprinus carpio*) TNF- α . *J Immunol* **183**:5319–
977 5332. doi:10.4049/jimmunol.0901780
- 978 García-Valtanen P, Martínez-López A, López-Muñoz A, Bello-Perez M, Medina-Gali RM, Ortega-
979 Villaizán MDM, Varela M, Figueras A, Mulero V, Novoa B, Estepa A, Coll J. 2017. Zebra fish
980 lacking adaptive immunity acquire an antiviral alert state characterized by upregulated gene
981 expression of apoptosis, multigene families, and interferon-related genes. *Front Immunol*
982 **8**:121. doi:10.3389/fimmu.2017.00121
- 983 Guegan F, Plazolles N, Baltz T, Coustou V. 2013. Erythrophagocytosis of desialylated red blood cells
984 is responsible for anaemia during Trypanosomavivax infection. *Cell Microbiol* **15**:1285–1303.
985 doi:10.1111/cmi.12123
- 986 Iraqi F, Sekikawa K, Rowlands J, Teale A. 2001. Susceptibility of tumour necrosis factor-alpha
987 genetically deficient mice to Trypanosoma congolense infection. *Parasite Immunol* **23**:445–
988 451.
- 989 Islam A, Woo P. 1991. Anemia and its mechanism in goldfish *Carassius auratus* infected with
990 Trypanosoma danilewskyi. *Dis Aquat Organ* **11**:37–43. doi:10.3354/dao011037
- 991 Joerink M, Groeneveld A, Ducro B, Savelkoul HFJ, Wiegertjes GF. 2007. Mixed infection with
992 Trypanoplasma borreli and Trypanosoma carassii induces protection: Involvement of cross-
993 reactive antibodies. *Dev Comp Immunol* **31**:903–915. doi:10.1016/j.dci.2006.12.003
- 994 Joerink M, Saeij J, Stafford J, Belosevic M, Wiegertjes G. 2004. Animal models for the study of
995 innate immunity: protozoan infections in fish In: Flik G, Wiegertjes GF, editors. *Host-Parasite*
996 *Interactions*. Taylor & Francis. p. (55):67–89.
- 997 Kaushik RS, Uzonna JE, Gordon JR, Tabel H. 1999. Innate resistance to Trypanosoma congolense
998 infections: Differential production of nitric oxide by macrophages from susceptible BALB/c and
999 resistant C57B1/6 mice. *Exp Parasitol* **92**:131–143. doi:10.1006/expr.1999.4408
- 1000 Kent M, Lom J, Dykova I, Dyková I. 1993. Protozoan Parasites of Fishes. *J Parasitol* **79**:673.
1001 doi:10.2307/3283600
- 1002 Kovacevic N, Hagen MO, Xie J, Belosevic M. 2015. The analysis of the acute phase response during
1003 the course of Trypanosoma carassii infection in the goldfish (*Carassius auratus* L.). *Dev Comp*
1004 *Immunol* **53**:112–122. doi:10.1016/j.dci.2015.06.009
- 1005 Krettli AU, Weisz-Carrington P, Nussenzweig RS. 1979. Membrane-bound antibodies to bloodstream
1006 Trypanosoma cruzi in mice: Strain differences in susceptibility to complement-mediated lysis.
1007 *Clin Exp Immunol* **37**:416–423.
- 1008 La Greca F, Haynes C, Stijlemans B, De Trez C, Magez S. 2014. Antibody-mediated control of
1009 Trypanosoma vivax infection fails in the absence of tumour necrosis factor. *Parasite Immunol*
1010 **36**:271–276. doi:10.1111/pim.12106
- 1011 Langenau DM, Ferrando AA, Traver D, Kutok JL, Hezel JP, Kanki JP, Zon LI, Look AT, Trede NS.
1012 2004. In vivo tracking of T cell development, ablation, and engraftment in transgenic
1013 zebrafish. *Proc Natl Acad Sci U S A* **101**:7369–7374.
- 1014 Lawson ND, Weinstein BM. 2002. In vivo imaging of embryonic vascular development using
1015 transgenic zebrafish. *Dev Biol* **248**:307–318. doi:10.1006/dbio.2002.0711
- 1016 LISCHKE A, KLEIN C, STIERHOF Y-D, HEMPEL M, MEHLERT A, ALMEIDA IC, FERGUSON MAJ,
1017 OVERATH P. 2000. Isolation and characterization of glycosylphosphatidylinositol-anchored,
1018 mucin-like surface glycoproteins from bloodstream forms of the freshwater-fish parasite
1019 Trypanosoma carassii. *Biochem J* **345**:693. doi:10.1042/0264-6021:3450693
- 1020 López-Muñoz RA, Molina-Berríos A, Campos-Estrada C, Abarca-Sanhueza P, Urrutia-Llancaqueo L,
1021 Peña-Espinoza M, Maya JD. 2018. Inflammatory and Pro-resolving Lipids in Trypanosomatid
1022 Infections: A Key to Understanding Parasite Control. *Front Microbiol* **9**:1961.
1023 doi:10.3389/fmicb.2018.01961
- 1024 Lopez R, Demick KP, Mansfield JM, Paulnock DM. 2008. Type I IFNs Play a Role in Early Resistance,
1025 but Subsequent Susceptibility, to the African Trypanosomes. *J Immunol* **181**:4908–4917.
1026 doi:10.4049/jimmunol.181.7.4908

Macrophages and neutrophils response to trypanosome infections in zebrafish

- 1027 Lucas Rudolf, Magez S, De Leys R, Fransen L, Scheerlinck JP, Rampelberg M, Sablon E, De
1028 Baetselier P. 1994. Mapping the lectin-like activity of tumor necrosis factor. *Science (80-)*
1029 **263**:814–817. doi:10.1126/science.8303299
- 1030 Lucas R, Magez S, De Leys R, Fransen L, Scheerlinck JP, Rampelberg M, Sablon E, De Baetselier P.
1031 1994. Mapping the lectin-like activity of tumor necrosis factor. *Science (80-)* **263**:814–817.
1032 Magez S., Lucas R, Darji A, Bajyana Songa E, Hamers R, Baetselier P de. 1993. Murine tumour
1033 necrosis factor plays a protective role during the initial phase of the experimental infection
1034 with *Trypanosoma brucei*. *Parasite Immunol* **15**:635–641. doi:10.1111/j.1365-
1035 3024.1993.tb00577.x
- 1036 Magez S, Caljon G. 2011. Mouse models for pathogenic African trypanosomes: unravelling the
1037 immunology of host-parasite-vector interactions. *Parasite Immunol* **33**:423–429.
1038 doi:10.1111/j.1365-3024.2011.01293.x
- 1039 Magez S, Geuskens M, Beschin A, del Favero H, Verschuere H, Lucas R, Pays E, de Baetselier P.
1040 1997. Specific uptake of tumor necrosis factor- α is involved in growth control of
1041 *Trypanosoma brucei*. *J Cell Biol* **137**:715–727.
- 1042 Magez S, Radwanska M, Beschin A, Sekikawa K, De Baetselier P. 1999. Tumor necrosis factor alpha
1043 is a key mediator in the regulation of experimental *Trypanosoma brucei* infections. *Infect*
1044 *Immun* **67**:3128–3132.
- 1045 Magez S, Radwanska M, Drennan M, Fick L, Baral TN, Allie N, Jacobs M, Nedospasov S, Brombacher
1046 F, Ryffel B, Baetselier P De. 2007. Tumor Necrosis Factor (TNF) Receptor-1 (TNFp55) Signal
1047 Transduction and Macrophage-Derived Soluble TNF Are Crucial for Nitric Oxide-Mediated
1048 *Trypanosoma congolense* Parasite Killing. *J Infect Dis* **196**:954–962. doi:10.1086/520815
- 1049 Magez S, Radwanska M, Drennan M, Fick L, Baral TN, Brombacher F, De Baetselier P. 2006.
1050 Interferon- γ and nitric oxide in combination with antibodies are key protective host
1051 immune factors during *Trypanosoma congolense* Tc13 Infections. *J Infect Dis* **193**:1575–
1052 1583.
- 1053 Magez S, Radwanska M, Stijlemans B, Xong H V, Pays E, De Baetselier P. 2001. A conserved
1054 flagellar pocket exposed high mannose moiety is used by African trypanosomes as a host
1055 cytokine binding molecule. *J Biol Chem* **276**:33458–33464.
- 1056 Magez S, Stijlemans B, Baral T, De Baetselier P. 2002. VSG-GPI anchors of African trypanosomes:
1057 their role in macrophage activation and induction of infection-associated immunopathology.
1058 *Microbes Infect* **4**:999–1006. doi:10.1016/S1286-4579(02)01617-9
- 1059 Magez S, Stijlemans B, De Baetselier P, Radwanska M, Pays E, Ferguson MAJ. 1998. The glycosyl-
1060 inositol-phosphate and dimyristoylglycerol moieties of the glycosylphosphatidylinositol anchor
1061 of the trypanosome variant-specific surface glycoprotein are distinct macrophage-activating
1062 factors. *J Immunol*.
- 1063 Mansfield JM, Paulnock DM. 2005. Regulation of innate and acquired immunity in African
1064 trypanosomiasis. *Parasite Immunol* **27**:361–371. doi:10.1111/j.1365-3024.2005.00791.x
- 1065 McAllister M, Phillips N, Belosevic M. 2019. *Trypanosoma carassii* infection in goldfish (*Carassius*
1066 *auratus* L.): changes in the expression of erythropoiesis and anemia regulatory genes.
1067 *Parasitol Res* **118**:1147–1158. doi:10.1007/s00436-019-06246-5
- 1068 Melo RC., Machado CR. 2001. *Trypanosoma cruzi*: Peripheral Blood Monocytes and Heart
1069 Macrophages in the Resistance to Acute Experimental Infection in Rats. *Exp Parasitol* **97**:15–
1070 23. doi:10.1006/EXPR.2000.4576
- 1071 Melo RCN, D'Ávila H, Fabrino DL, Almeida PE, Bozza PT. 2003. Macrophage lipid body induction by
1072 Chagas disease in vivo: putative intracellular domains for eicosanoid formation during
1073 infection. *Tissue Cell* **35**:59–67. doi:10.1016/S0040-8166(02)00105-2
- 1074 Melo RCN, Fabrino DL, Dias FF, Parreira GG. 2006. Lipid bodies: Structural markers of
1075 inflammatory macrophages in innate immunity. *Inflamm Res* **55**:342–348.
1076 doi:10.1007/s00011-006-5205-0
- 1077 Mishra RR, Senapati SK, Sahoo SC. 2017. Trypanosomiasis induced oxidative stress and hemato-
1078 biochemical alteration in cattle. *Artic J Entomol Zool Stud* **5**:721–727.
- 1079 Musoke AJ, Barbet AF. 1977. Activation of complement by variant-specific surface antigen of
1080 *Trypanosoma brucei*. *Nature* **270**:438–440.
- 1081 Naessens J. 2006. Bovine trypanotolerance: A natural ability to prevent severe anaemia and
1082 haemophagocytic syndrome? *Int J Parasitol* **36**:521–528. doi:10.1016/j.ijpara.2006.02.012
- 1083 Namangala B, De Baetselier P, Beschin A. 2009. Both Type-I and Type-II Responses Contribute to
1084 Murine Trypanotolerance. *J Vet Med Sci* **71**:313–318.
- 1085 Namangala B, Noel W, De Baetselier P, Brys L, Beschin A. 2001. Relative contribution of interferon-
1086 gamma and interleukin-10 to resistance to murine African trypanosomiasis. *J Infect Dis*
1087 **183**:1794–1800.
- 1088 Nguyen-Chi M, Laplace-Builhé B, Travnickova J, Luz-Crawford P, Tejedor G, Lutfalla G, Kissa K,
1089 Jorgensen C, Djouad F. 2017. TNF signaling and macrophages govern fin regeneration in

Macrophages and neutrophils response to trypanosome infections in zebrafish

- 1090 zebrafish larvae. *Cell Death Dis* **8**:e2979–e2979. doi:10.1038/cddis.2017.374
- 1091 Nguyen-Chi M, Laplace-Builhe B, Travnickova J, Luz-Crawford P, Tejedor G, Phan QT, Duroux-
- 1092 Richard I, Levraud J-P, Kissa K, Lutfalla G, Jorgensen C, Djouad F. 2015. Identification of
- 1093 polarized macrophage subsets in zebrafish. *Elife* **4**:e07288. doi:10.7554/eLife.07288
- 1094 Nguyen-Chi M, Phan QT, Gonzalez C, Dubremetz J-F, Levraud J-P, Lutfalla G. 2014a. Transient
- 1095 infection of the zebrafish notochord with *E. coli* induces chronic inflammation. *Dis Model Mech*
- 1096 **7**:871–82. doi:10.1242/dmm.014498
- 1097 Nguyen-Chi M, Phan QT, Gonzalez C, Dubremetz J-F, Levraud J-P, Lutfalla G. 2014b. Transient
- 1098 infection of the zebrafish notochord with *E. coli* induces chronic inflammation. *Dis Model Mech*
- 1099 **7**:871–82. doi:10.1242/dmm.014498
- 1100 Noël W, Hassanzadeh G, Raes G, Namangala B, Daems I, Brys L, Brombacher F, Baetselier PD,
- 1101 Beschin A. 2002. Infection stage-dependent modulation of macrophage activation in
- 1102 *Trypanosoma congolense*-resistant and -susceptible mice. *Infect Immun* **70**:6180–6187.
- 1103 Noël W, Raes G, Ghassabeh GH, De Baetselier P, Beschin A. 2004. Alternatively activated
- 1104 macrophages during parasite infections. *Trends Parasitol* **20**:126–133.
- 1105 doi:10.1016/j.pt.2004.01.004
- 1106 O’Gorman GM, Park SDE, Hill EW, Meade KG, Mitchell LC, Agaba M, Gibson JP, Hanotte O,
- 1107 Naessens J, Kemp SJ, MacHugh DE. 2006. Cytokine mRNA profiling of peripheral blood
- 1108 mononuclear cells from trypanotolerant and trypanosusceptible cattle infected with
- 1109 *Trypanosoma congolense*. *Physiol Genomics* **28**:53–61.
- 1110 doi:10.1152/physiolgenomics.00100.2006
- 1111 Oladiran A, Beauparlant D, Belosevic M. 2011. The expression analysis of inflammatory and
- 1112 antimicrobial genes in the goldfish (*Carassius auratus* L.) infected with *Trypanosoma carassii*.
- 1113 *Fish Shellfish Immunol* **31**:606–613. doi:10.1016/j.fsi.2011.07.008
- 1114 Oladiran A, Belosevic M. 2012. Recombinant glycoprotein 63 (Gp63) of *Trypanosoma carassii*
- 1115 suppresses antimicrobial responses of goldfish (*Carassius auratus* L.) monocytes and
- 1116 macrophages q. *Int J Parasitol* **42**:621–633. doi:10.1016/j.ijpara.2012.04.012
- 1117 Oladiran A, Belosevic M. 2010. *Trypanosoma carassii* calreticulin binds host complement
- 1118 component C1q and inhibits classical complement pathway-mediated lysis. *Dev Comp*
- 1119 *Immunol* **34**:396–405. doi:10.1016/j.dci.2009.11.005
- 1120 Oladiran A, Belosevic M. 2009. *Trypanosoma carassii* hsp70 increases expression of inflammatory
- 1121 cytokines and chemokines in macrophages of the goldfish (*Carassius auratus* L.). *Dev Comp*
- 1122 *Immunol* **33**:1128–1136. doi:10.1016/j.dci.2009.06.003
- 1123 Overath P, Haag J, Lischke A, O’Hugin C. 2001. The surface structure of trypanosomes in relation
- 1124 to their molecular phylogeny. *Int J Parasitol* **31**:468–471.
- 1125 Overath P, Ruoff J, Stierhof YD, Haag J, Tichy H, Dyková I, Lom J. 1998. Cultivation of bloodstream
- 1126 forms of *Trypanosoma carassii*, a common parasite of freshwater fish. *Parasitol Res* **84**:343–
- 1127 347. doi:10.1007/s004360050408
- 1128 Page DM, Wittamer V, Bertrand JY, Lewis KL, Pratt DN, Delgado N, Schale SE, McGue C, Jacobsen
- 1129 BH, Doty A, Pao Y, Yang H, Chi NC, Magor BG, Traver D. 2013. An evolutionarily conserved
- 1130 program of B-cell development and activation in zebrafish. *Blood* **122**:e1–e11.
- 1131 doi:10.1182/blood-2012-12-471029
- 1132 Palha N, Guivel-Benhassine F, Briolat V, Lutfalla G, Sourisseau M, Ellett F, Wang CH, Lieschke GJ,
- 1133 Herbomel P, Schwartz O, Levraud JP. 2013. Real-Time Whole-Body Visualization of
- 1134 Chikungunya Virus Infection and Host Interferon Response in Zebrafish. *PLoS Pathog*
- 1135 **9**:e1003619. doi:10.1371/journal.ppat.1003619
- 1136 Petrie-Hanson L, Hohn C, Hanson L. 2009. Characterization of rag1 mutant zebrafish leukocytes.
- 1137 *BMC Immunol* **10**:8. doi:10.1186/1471-2172-10-8
- 1138 Phan QT, Sipka T, Gonzalez C, Levraud JP, Lutfalla G, Nguyen-Chi M. 2018. Neutrophils use
- 1139 superoxide to control bacterial infection at a distance. *PLoS Pathog* **14**:1–29.
- 1140 doi:10.1371/journal.ppat.1007157
- 1141 Radwanska M, Vereecke N, Deleuw V, Pinto J, Magez S. 2018. Salivarian Trypanosomiasis: A
- 1142 Review of Parasites Involved, Their Global Distribution and Their Interaction With the Innate
- 1143 and Adaptive Mammalian Host Immune System. *Front Immunol* **9**:1–20.
- 1144 doi:10.3389/fimmu.2018.02253
- 1145 Ramakrishnan L. 2013. The zebrafish guide to tuberculosis immunity and treatment. *Cold Spring*
- 1146 *Harb Symp Quant Biol* **78**:179–192. doi:10.1101/sqb.2013.78.023283
- 1147 Renshaw SA, Loynes CA, Trushell DMI, Elworthy S, Ingham PW, Whyte MKB. 2006. A transgenic
- 1148 zebrafish model of neutrophilic inflammation. *Blood* **108**:3976–3978. doi:10.1182/blood-
- 1149 2006-05-024075
- 1150 Renshaw SA, Trede NS. 2012. A model 450 million years in the making: zebrafish and vertebrate
- 1151 immunity. *Dis Model Mech* **5**:38–47. doi:10.1242/dmm.007138
- 1152 Ribeiro CMS, Pontes MJSL, Bird S, Chadzinska M, Scheer M, Verburg-van Kemenade BML,
- 1153 Savelkoul HFJ, Wiegertjes GF. 2010. Trypanosomiasis-induced Th17-like immune responses in

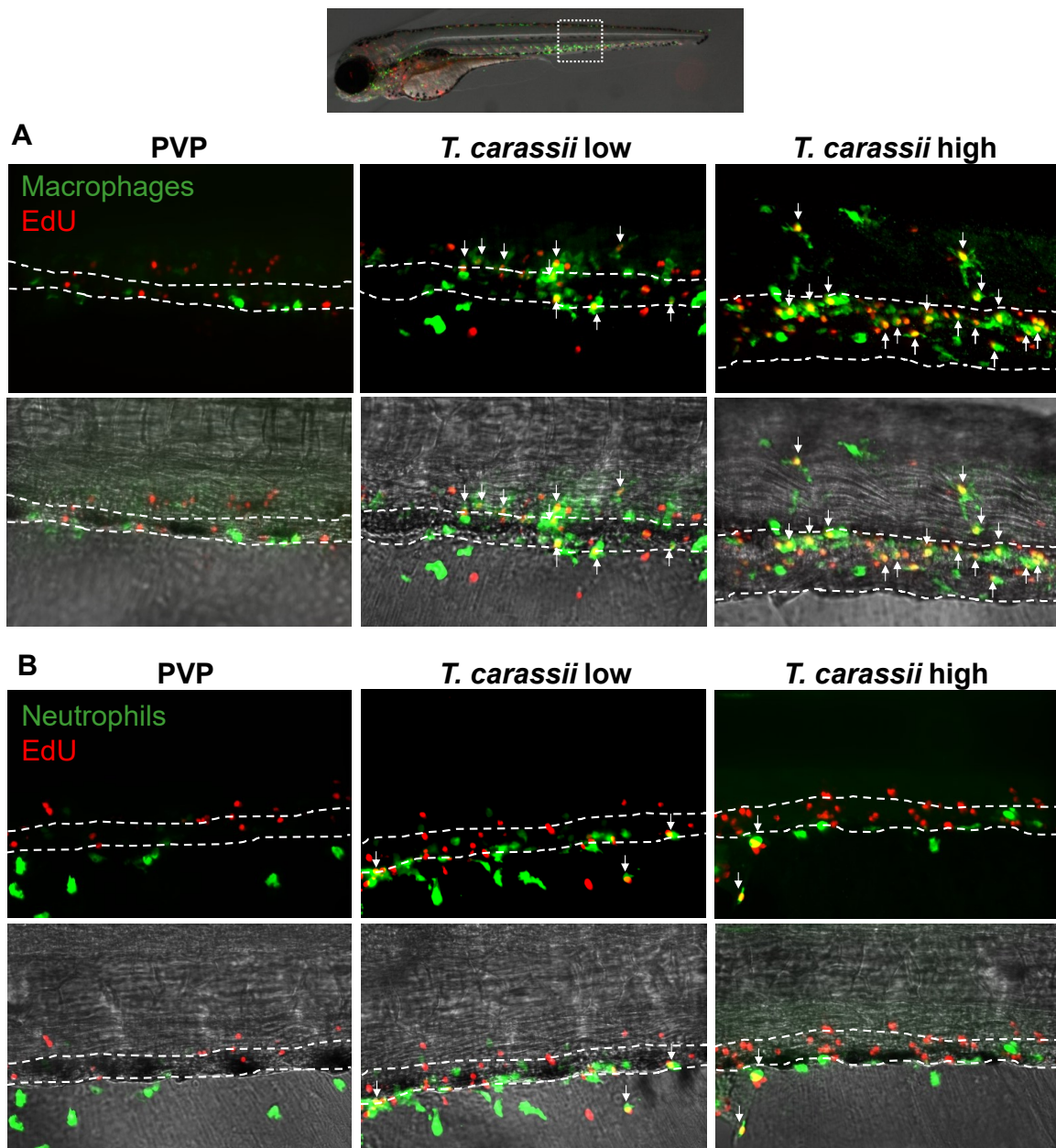
Macrophages and neutrophils response to trypanosome infections in zebrafish

- 1154 carp. *PLoS One* **5**:e13012. doi:10.1371/journal.pone.0013012
- 1155 Rifkin MR, Landsberger FR. 1990. Trypanosome variant surface glycoprotein transfer to target
- 1156 membranes: A model for the pathogenesis of trypanosomiasis. *Proc Natl Acad Sci U S A*
- 1157 **87**:801–805. doi:10.1073/pnas.87.2.801
- 1158 Rosowski EE, Knox BP, Archambault LS, Huttenlocher A, Keller NP, Wheeler RT, Davis JM. 2018.
- 1159 The zebrafish as a model host for invasive fungal infections. *J Fungi* **4**.
- 1160 doi:10.3390/jof4040136
- 1161 Russell DG, Cardona P-J, Kim M-J, Allain S, Altare F. 2009. Foamy macrophages and the
- 1162 progression of the human tuberculosis granuloma. *Nat Immunol* **10**:943–948.
- 1163 doi:10.1038/ni.1781
- 1164 Saeij JPJ, Groeneveld A, Van Rooijen N, Haenen OLM, Wiegertjes GF. 2003. Minor effect of
- 1165 depletion of resident macrophages from peritoneal cavity on resistance of common carp
- 1166 *Cyprinus carpio* to blood flagellates. *Dis Aquat Organ* **57**:67–75. doi:10.3354/dao057067
- 1167 Scharsack JP, Steinhagen D, Kleczka C, Schmidt JO, Körting W, Michael RD, Leibold W, Schuberth
- 1168 HJ. 2003. Head kidney neutrophils of carp (*Cyprinus carpio* L.) are functionally modulated by
- 1169 the haemoflagellate *Trypanoplasma borreli*. *Fish Shellfish Immunol* **14**:389–403.
- 1170 doi:10.1006/fsim.2002.0447
- 1171 Sileghem M, Saya R, Grab DJ, Naessens J. 2001. An accessory role for the diacylglycerol moiety of
- 1172 variable surface glycoprotein of African trypanosomes in the stimulation of bovine monocytes.
- 1173 *Vet Immunol Immunopathol* **78**:325–339. doi:10.1016/S0165-2427(01)00241-0
- 1174 Simpson AGB, Stevens JR, Lukes J. 2006. The evolution and diversity of kinetoplastid flagellates.
- 1175 *Trends Parasitol* **22**:168–174.
- 1176 Sternberg JM, Mabbott NA. 1996. Nitric oxide-mediated suppression of T cell responses during
- 1177 *Trypanosoma brucei* infection: Soluble trypanosome products and interferon- γ are synergistic
- 1178 inducers of nitric oxide synthase. *Eur J Immunol*. doi:10.1002/eji.1830260306
- 1179 Stijlemans B, Caljon G, Van Den Abbeele J, Van Ginderachter JA, Magez S, De Trez C. 2016.
- 1180 Immune evasion strategies of *Trypanosoma brucei* within the mammalian host: Progression to
- 1181 pathogenicity. *Front Immunol*. doi:10.3389/fimmu.2016.00233
- 1182 Stijlemans B, Williams M, Raes G, Beschin A, Magez S, De Baetselier P. 2007. African
- 1183 trypanosomiasis: from immune escape and immunopathology to immune intervention. *Vet*
- 1184 *Parasitol* **148**:3–13.
- 1185 Stijlemans B, Radwanska M, Trez C De, Magez S. 2017. African trypanosomes undermine humoral
- 1186 responses and vaccine development: Link with inflammatory responses? *Front Immunol*
- 1187 **8**:582. doi:10.3389/fimmu.2017.00582
- 1188 Torraca V, Masud S, Spaik HP, Meijer AH. 2014. Macrophage-pathogen interactions in infectious
- 1189 diseases: new therapeutic insights from the zebrafish host model. *Dis Model Mech* **7**:785–
- 1190 797. doi:10.1242/dmm.015594
- 1191 Torraca V, Mostowy S. 2018. Zebrafish Infection: From Pathogenesis to Cell Biology. *Trends Cell*
- 1192 *Biol* **28**:143–156. doi:10.1016/j.tcb.2017.10.002
- 1193 Travnickova J, Tran Chau V, Julien E, Mateos-Langerak J, Gonzalez C, Lelievre E, Lutfalla G, Tavian
- 1194 M, Kissa K. 2015. Primitive macrophages control HSPC mobilization and definitive
- 1195 haematopoiesis. *Nat Commun* **6**:6227. doi:10.1038/ncomms7227
- 1196 Vallochi AL, Teixeira L, Oliveira K da S, Maya-Monteiro CM, Bozza PT. 2018. Lipid Droplet, a Key
- 1197 Player in Host-Parasite Interactions. *Front Immunol* **9**:1022. doi:10.3389/fimmu.2018.01022
- 1198 White RM, Sessa A, Burke C, Bowman T, LeBlanc J, Ceol C, Bourque C, Dovey M, Goessling W,
- 1199 Burns CE, Zon LI. 2008. Transparent Adult Zebrafish as a Tool for In Vivo Transplantation
- 1200 Analysis. *Cell Stem Cell*. doi:10.1016/j.stem.2007.11.002
- 1201 Woo PTK, Ardelli BF. 2014. Immunity against selected piscine flagellates. *Dev Comp Immunol*
- 1202 **43**:268–279. doi:10.1016/j.dci.2013.07.006
- 1203 Wu H, Liu G, Shi M. 2017. Interferon gamma in African trypanosome infections: Friends or foes?
- 1204 *Front Immunol*. doi:10.3389/fimmu.2017.01105
- 1205 Wymann MP, Schneider R. 2008. Lipid signalling in disease. *Nat Rev Mol Cell Biol*.
- 1206 doi:10.1038/nrm2335
- 1207

Macrophages and neutrophils response to trypanosome infections in zebrafish

1208 **Supplementary files**

1209



1210

1211

1212

1213

1214

1215

1216

1217

1218

S1 Fig. Differential distribution of EdU⁺ macrophages and neutrophils along the caudal vein of high- and low-infected larvae. Zebrafish were treated as described in figure 5. **A)** A high number of macrophages can be seen around and inside the caudal vein. Especially in high-infected individuals, the majority of cells within the vessel was EdU⁺, suggesting that in these larvae, proliferating macrophages migrated to the vessels. **B)** Neutrophils were never observed within the caudal vein and, independently of whether they proliferated (EdU⁺) or not, were mostly observed lining the vessel.

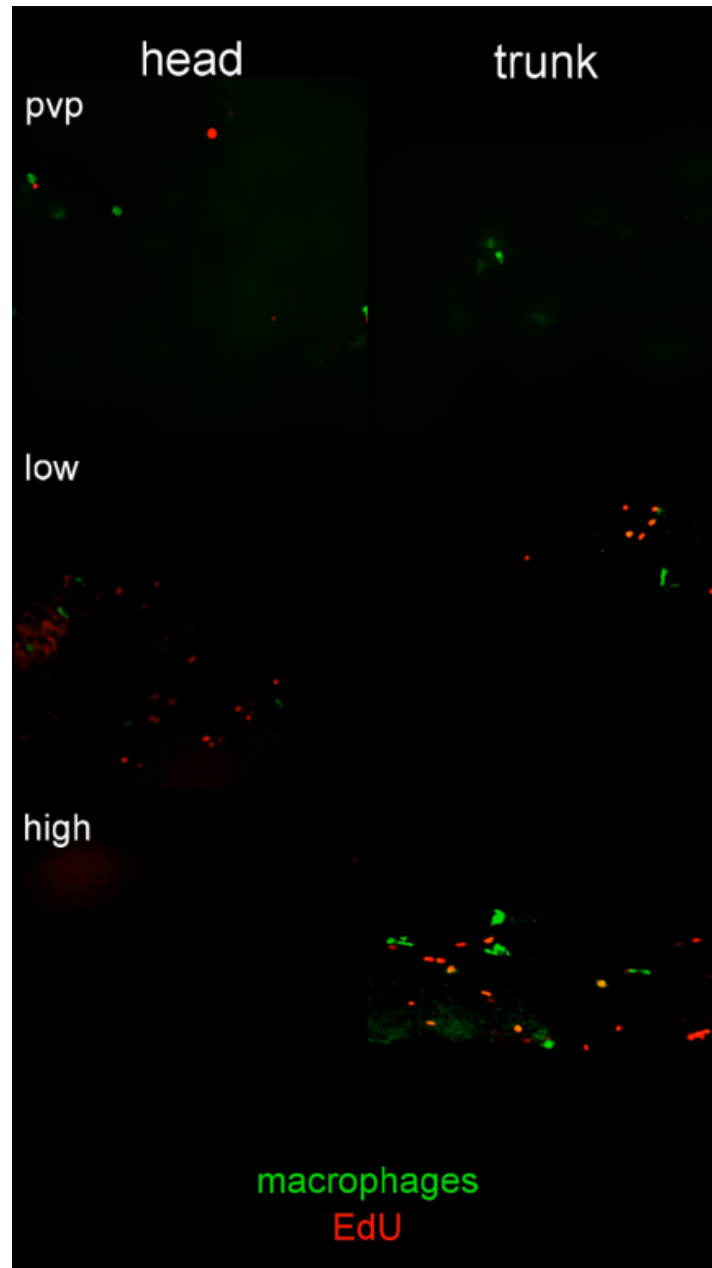
Macrophages and neutrophils response to trypanosome infections in zebrafish

1219

Representative movie fragments of
trypanosome detection in ISCs
and
trypanosome extravasation at various locations
in high- or low-infected zebrafish larvae

S1 Video. Clinical signs of *T. carassii* infection in high- and low-infected zebrafish larvae. *Tg(mpeg1.4:mCherry-F;mpx:GFP)* 5 dpf zebrafish were injected with $n=200$ *T. carassii* or with PVP and imaged at various time points after infection. Shown are high-speed videos (500 frames/sec, fps) or real-time videos (20 fps) capturing trypanosomes *in vivo* in blood or in tissues, as well as describing typical signs of anaemia and vasodilation.

Macrophages and neutrophils response to trypanosome infections in zebrafish

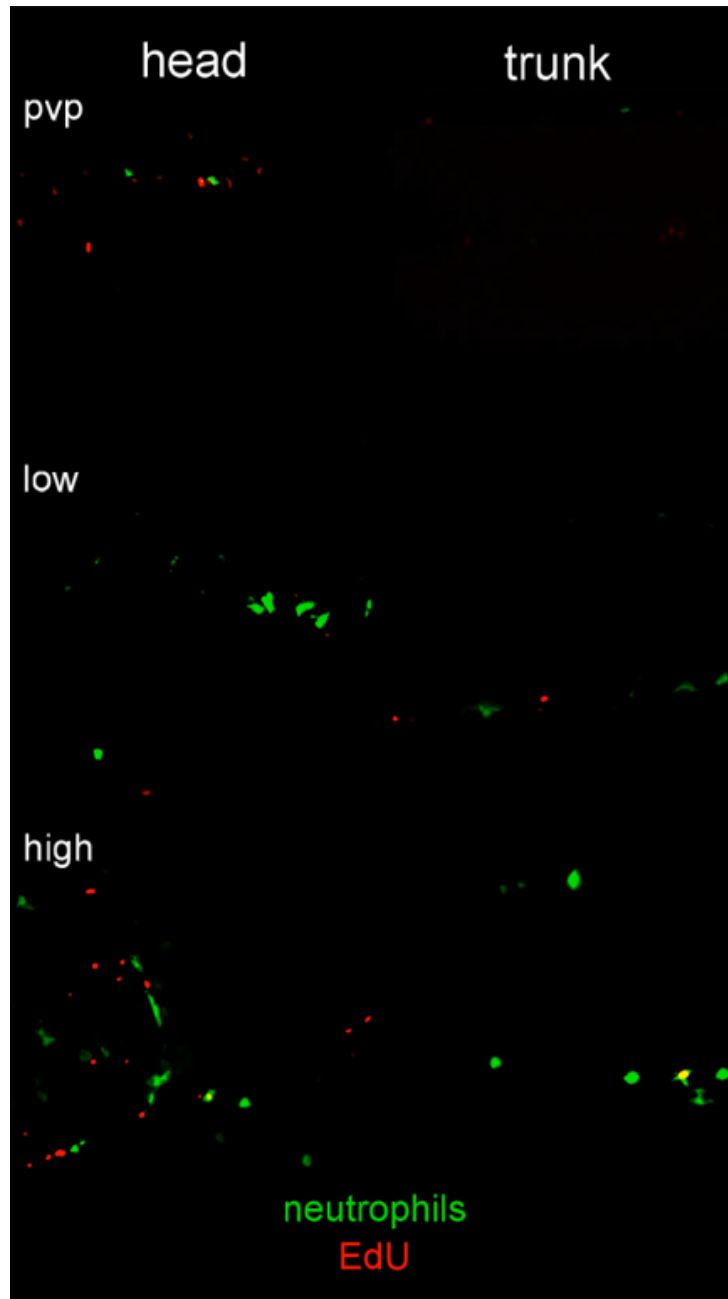


1235

1236

1237 **S2 video. *T. carassii* infection triggers macrophage proliferation.** AVI files corresponding to
1238 the maximum projection images shown in figure 5; Arrows are positioned as in figure 5, and indicate
1239 the location of EdU⁺ macrophages

Macrophages and neutrophils response to trypanosome infections in zebrafish

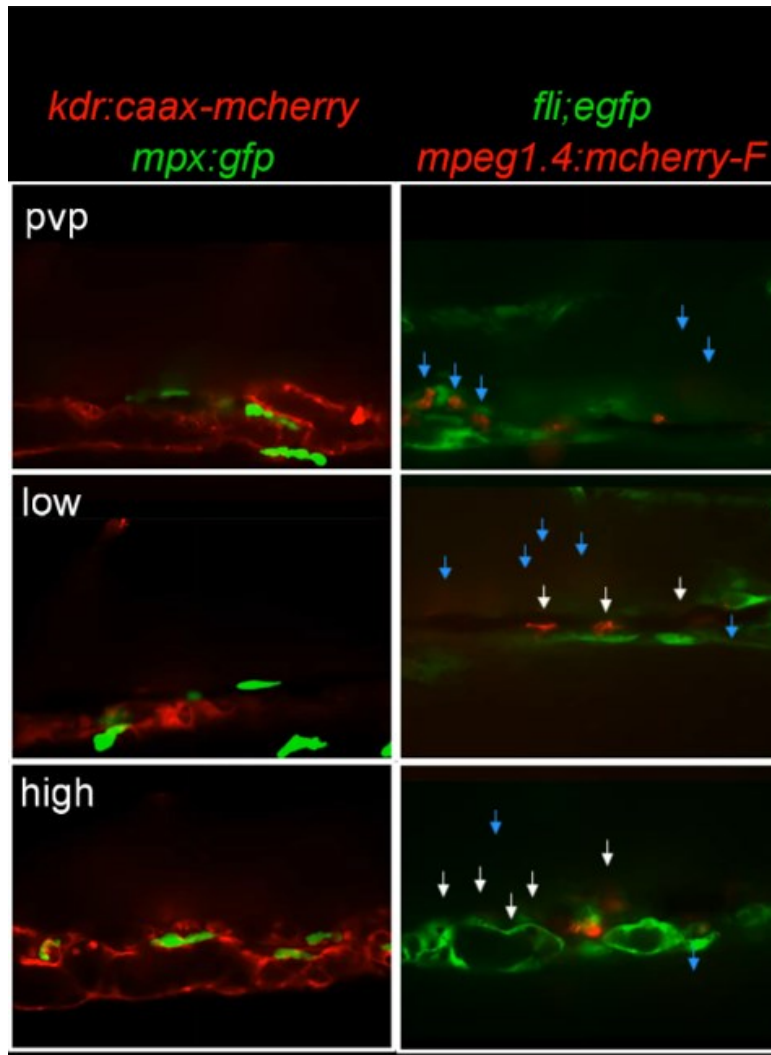


1240

1241

1242 **S3 video. *T. carassii* infection triggers neutrophils proliferation.** AVI files corresponding to the
1243 maximum projection images shown in figure 6; Arrows are positioned as in figure 6, and indicate the
1244 location of EdU⁺ neutrophils

Macrophages and neutrophils response to trypanosome infections in zebrafish



1245

1246

1247

1248

1249

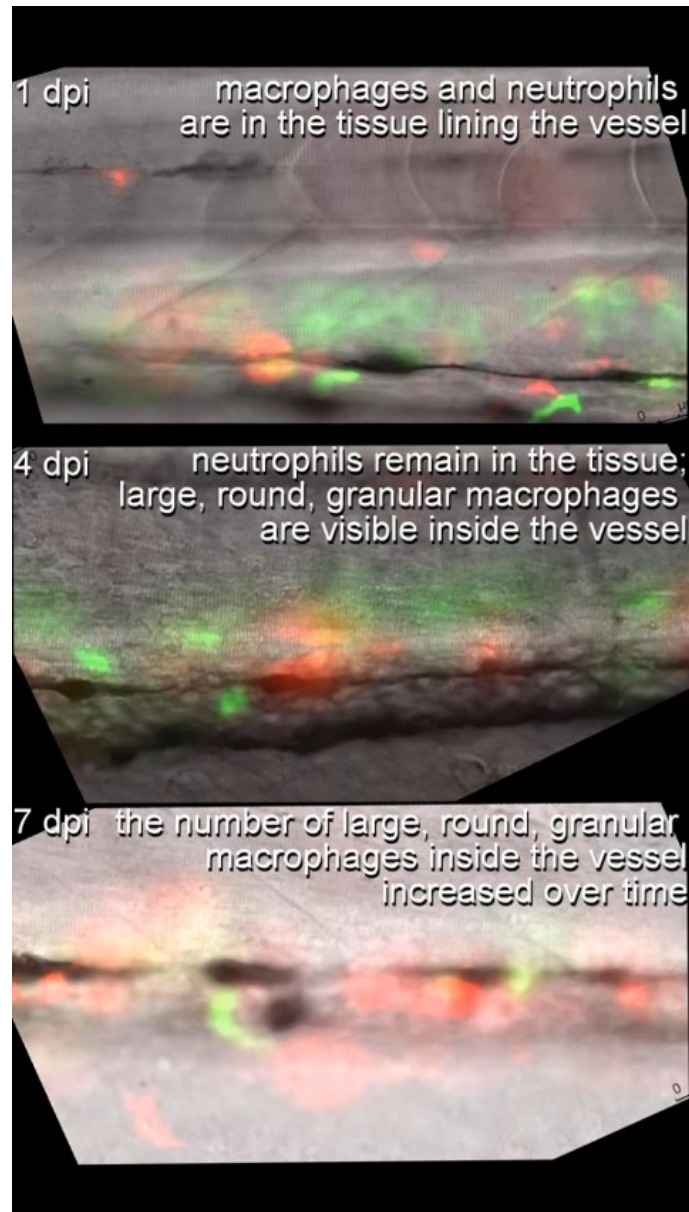
1250

1251

1252

S4 Video. Macrophages are recruited into the cardinal caudal vein of high-infected zebrafish larvae. Zebrafish larvae were treated and imaged as described in figure 7. Shown are the AVI files corresponding to the maximum projection images shown in figure 7; Neutrophils were never observed within the vessel independently of the infection level (left panels). Macrophages however, could be seen outside (blue arrows) and inside the vessel (white arrows). The number of rounded macrophages inside the vessel increased with the infection level.

Macrophages and neutrophils response to trypanosome infections in zebrafish



1253

1254

1255

1256 **S5 Video. The occurrence of large granular macrophages increases with the progression**

1257 **of the infection in high-infected individuals.** *Tg(mpeg1.4:mCherry-F;mpx:GFP)* zebrafish larvae

1258 were injected intravenously at 5 dpf with n=200 *T. carassii* or with PVP. At 4 dpi larvae were

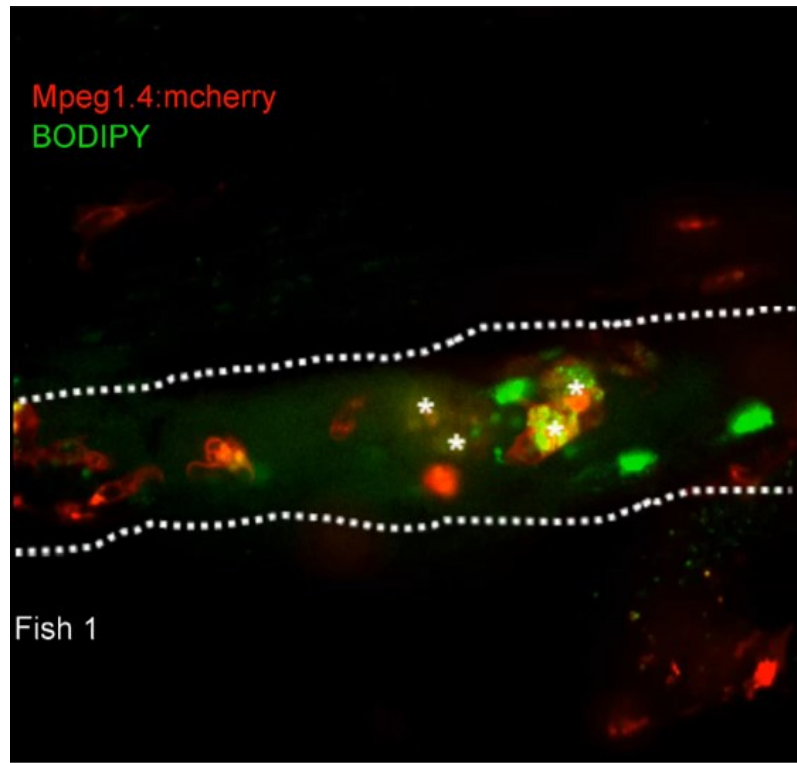
1259 separated into high- and low-infected individuals and imaged at 5 dpi with a DMi8 inverted digital

1260 Leica microscope. The occurrence of large macrophages (arrows) in the cardinal caudal vessel

1261 increased with the progression of the infection and was exclusive to high infected individuals (4 and

7 dpi).

Macrophages and neutrophils response to trypanosome infections in zebrafish



1262

1263

1264

1265

1266

1267

1268

1269

1270

S6 Video. Large granular macrophages inside the vessel of high-infected larvae are rich in lipid bodies. *Tg(mpeg1.4:mCherry-F)* zebrafish larvae were infected intravenously at 5 dpf with $n=200$ *T. carassii* or with PVP. At 3 dpi, larvae received 1 nl of 30 μ M BODIPY-FLC5 and were imaged 18–20 hours later using a Roper Spinning Disc Confocal Microscope at a 40x magnification. The AVI files corresponding to the maximum projection images shown in figure 8, as well as a second individual, are shown. Asterisks indicate the position of foamy macrophages inside the caudal vessel (dashed line).